AD_____

Award Number: W81XWH-04-2-0022

TITLE: Development of a Multileaf Collimator for Proton Radiotherapy

PRINCIPAL INVESTIGATOR: Zelig Tochner, M.D.

CONTRACTING ORGANIZATION: University of Pennsylvania
Philadelphia PA 19104-6205

REPORT DATE: June 2012

TYPE OF REPORT: Annual

PREPARED FOR: U.S. Army Medical Research and Materiel Command
Fort Detrick, Maryland 21702-5012

DISTRIBUTION STATEMENT: Approved for Public Release;
Distribution Unlimited

REPORT DOCUMENTATION PAGE

Form Approved
OMB No. 0704-0188

1. REPORT DATE	**2. REPORT TYPE**	**3. DATES COVERED**
June 2012	Annual	17 May 2011 – 16 May 2012

4. TITLE AND SUBTITLE

Development of a Multileaf Collimator for Proton Radiotherapy

5a. CONTRACT NUMBER

5b. GRANT NUMBER
W81XWH-04-2-0022

5c. PROGRAM ELEMENT NUMBER

6. AUTHOR(S)

Zelig Tochner M.D., James McDonough Ph.D., Derek Dolney Ph.D., Neha Vapiwala M.D., Ramesh Rengan M.D., Ph.D.

E-Mail: tochner@uphs.upenn.edu

5d. PROJECT NUMBER

5e. TASK NUMBER

5f. WORK UNIT NUMBER

7. PERFORMING ORGANIZATION NAME(S) AND ADDRESS(ES)

University of Pennsylvania
Philadelphia PA 19104-6205

8. PERFORMING ORGANIZATION REPORT NUMBER

9. SPONSORING / MONITORING AGENCY NAME(S) AND ADDRESS(ES)
U.S. Army Medical Research and Materiel Command
Fort Detrick, Maryland 21702-5012

10. SPONSOR/MONITOR'S ACRONYM(S)

11. SPONSOR/MONITOR'S REPORT NUMBER(S)

12. DISTRIBUTION / AVAILABILITY STATEMENT
Approved for Public Release; Distribution Unlimited

13. SUPPLEMENTARY NOTES

14. ABSTRACT

This report is the annual report for Phase one, out of three phases, of a DOD grant that was given to UPENN and Walter Reed Medical center to develop Proton Therapy center. This report describes the seventh year of a project to design and construct multileaf collimators (MLC) to be used in proton radiotherapy, the sixth year of the project to develop scanned beam technology for proton radiotherapy, and the fifth year of the project to develop image guided treatment protocols for proton therapy. This research project is a joint collaborative effort between the University of Pennsylvania (HUP) and the Walter Reed Army Medical Center (WRAMC), and is part of a larger project to build a state-of-the-art proton radiotherapy facility in Philadelphia. The accomplishments during the past year of the project are described in this report.

15. SUBJECT TERMS
Radiation Oncology, Proton Therapy, Multileaf Collimator, MLC, Conformal Radiotherapy

16. SECURITY CLASSIFICATION OF:			**17. LIMITATION OF ABSTRACT**	**18. NUMBER OF PAGES**	**19a. NAME OF RESPONSIBLE PERSON**
					USAMRMC
a. REPORT	**b. ABSTRACT**	**c. THIS PAGE**			**19b. TELEPHONE NUMBER** *(include area code)*
U	U	U	UU	48	

Table of Contents

Introduction

This report is the annual report for Phase 1 –out of three phases – of a DOD grant that was given to UPENN and WRAMC for the development of proton therapy facility and associated equipment and research.

The overall goal of this multi-year research project in collaboration with the Walter Reed Army Medical Center is to develop the necessary technology to make the proton facility that is being constructed in Philadelphia the most advanced proton radiotherapy center. The first technology is the development of a multileaf collimator (MLC) for proton therapy and investigates the issues that must be resolved to use an MLC in proton therapy. The second technology under study is the optimization of the spot-scanning delivery technique including the effects of organ motion. The third technology is the development of protocols to apply the techniques of image-guided and adaptive radiotherapy to proton therapy, and to develop a decision-making algorithm to maximize the efficiency of the facility. This report describes the progress during the sixth –seventh year of the expected seven-year process. Included in that progress are the following activities and achievements: (1) Use of the GEANT4 Monte Carlo code, which was developed in the previous years of the project, to test various MLC designs, culminating in the delivery of the first MLC and the status of the on-going tests of that MLC; (2) Use of the same simulation program to optimize the dose distribution from scanned beams accounting for inhomogeneities and organ motion; (3) Development of treatment protocols and an understanding of the factors that are involved to efficiently utilize the beam; and (4) Advancement of the interconnectivity between the department at Penn and the Walter Reed Army Medical Center to permit remote treatment planning.

Body

In June 2006, following years of defining specifications and evaluating proposals, the University of Pennsylvania Health System (UPHS) signed a contract with Ion Beam Applications, S.A. (IBA). In addition to the details associated with the delivery of a proton therapy system the contract included three development agreements directly related to the work supported by this grant to develop technology for proton therapy. The development agreements between UPHS, IBA and Varian Medical Systems, Inc. (the leading conventional radiotherapy vendor) were: (1) to develop a multileaf collimator for the IBA proton delivery system, (2) to develop a cone-beam CT to permit imaging of the patient in the treatment room, and (3) to develop the pencil-beam scanning algorithm of the Varian treatment planning system.

Much of the effort in the past year has been to: (1) test the final MLC; (2) design a system that permits the treatment of shallow targets with scanned beams; (3) continue to enroll patients on adaptive radiotherapy study (4) Expand capabilities of treating additional body sites and develop additional treatment protocols and submit them to regulatory bodies for approval while expanding the collaboration with Walter Reed Military Medical Center (WRMMC) in these areas. To that end UPHS personnel have met with IBA and Varian engineers multiple times and have teleconferences or WebEx-type remote meetings nearly every week. The MLC, which has the highest priority because the treatment rooms cannot be commissioned without it, is the most advanced of these projects. The scanning development is close to completion; the clinical implementation had been delayed by approximately one to two years because we did not feel that the IBA system was mature enough for routine clinical use. The cone-beam CT development has made the least progress thus far, but we are expecting an installation of the first prototype later this year after we reached an agreement with IBA on development of a product which will use some of the existing imaging technology that is already in use in our proton gantries. Cone-beam CT technology has only recently been introduced to conventional radiotherapy and is constantly being upgraded. Our challenge is to design a device that will be able to easily follow the advances the system makes in conventional therapy.

This report concentrates on the sixth year achievements of the multileaf collimator development, the fifth year of work on the spot-scanning/motion project, and the fourth year on the development of image-guided and adaptive radiotherapy protocols. The Statement of Work in the approved grant proposals included the following items to be investigated. (Note: to minimize confusion, the years in which we expected to perform the work have been replaced by the fiscal year because there are three separate starting dates.) Because of the delay in choosing the vendor and the delay in the development by the vendor of some of the technologies several of the aims that were originally planned to be completed by now, are still ongoing. The current schedule is such that the fifth treatment room (Proton 2 with pencil beam scanning) was commissioned in late 2011. The items in the Statement of Work are listed below with a comment on the status of any item that was to have work performed by this time.

The projects identified included:

1. Multileaf collimator (MLC) for use on proton therapy gantries
2. Cone Beam CT (CBCT) on the proton gantry for localization of target volumes
3. Proton Radiography to determine dose and stopping power of various tissues
4. Positron Emission Tomography (PET) imaging on the gantry to evaluate dose deposition within tissues irradiated

5. Pencil Beam Scanning (PBS) proton beam using adaptive radiotherapy techniques based on implementation of MLC, Cone Beam CT, and PET imaging

Phase One- All the action items in the SOW for phase one were completed by us with minimal adjustments in some of the items that were required by the development of the proton system.

Phase Two- The SOW for phase two included mostly the development and implementation of Pencil Beam Scanning, and development of joint military UPENN telemedicine system. The delivery and installation of clinical PBS system by our contractor- IBA- was completed during this past year for the fixed beam room and patient treatments were begun in November 2011. Work is on-going to prove Gantries 1 & 3 with that same technology.

Phase Three- The SOW included studying of imaging modalities for proton, development of CBCT, studying and development of adaptive proton therapy which is based on repeated imaging during proton therapy and development of smart scheduling system.
The studies of imaging modalities per the SOW were done.
During the past year we entered into an agreement with IBA to develop together a CBCT system for use in the IBA gantries. We expect delivery of components during the autumn 2012.
To satisfy the SOW regarding adaptive radiotherapy for proton we have developed IRB approved protocol which is currently being reviewed by the DOD. Once approved we will recruit the additional personal needed to execute it. (see attached budget)

We continue to develop the smart scheduling system as part of phase 5 (W81XWH-07-2-0121).

MLC Development

1. Leaf design: (FY 2005). This is complete – the final design has been incorporated into the GEANT4 simulation as described in Section I.A.1.

2. Joint Military/Civilian Proton Radiotherapy Center: (FY 2005-2006). The first stage of this was completed in 2007. A more complete system is part of phase 2.

3. Investigate the design factors affecting the lateral penumbra of the beam: -completed- (FY 2005).

4. Design of the MLC system: (FY 2005). This is complete. The MLC is in clinical use and two papers are being written to describe the design and clinical performance of the device.

5. Production of a prototype MLC and initial testing: (FY 2006). The prototype was tested at the Jacksonville proton facility in September 2008.

6. Incorporation of the MLC design into the treatment planning system: (FY 2006). This work is essentially finished. We had some comments/suggestions regarding the graphics in the treatment planning system that the Varian software engineers are looking into.

7. Production of MLCs for gantry and fixed-beam rooms: (FY 2007-2009). The first MLC arrived in February 2009 and the others over the following year. The fixed-beam room does not use an MLC.

8. Commissioning MLCs for gantry and fixed-beam rooms: (FY 2007-2009). All four MLCs are commissioned.

9. Adapt the system to include collimation on a layer-by-layer basis: (FY 2007-2009). This work began in the summer of 2009 and is still being investigated.

Spot-Scanning Development

1. Scan optimization: (FY 2006). This work began in 2006 and is continuing. The current status is detailed in Section II. Most of the recent work is focused on the model used in the Eclipse treatment planning system.

2. Patient motion simulation: (FY 2006-2007). We have installed a breath-hold system and tested it on the conventional radiotherapy side of the department and are in the process of adapting it for protons. We expect that will happen during the summer / autumn 2012.

3. Development of phantom for motion studies: (FY 2007-2008). We decided to purchase a phantom for motion studies rather than building one ourselves.

4. Development of dosimetry systems for scanned beams: (FY 2006-2009). As described in Section I of this report, we are developing a 3D detector based on technology used at CERN.

5. Production of beam scanning nozzle and initial testing: (FY 2008-2010). We commissioned the fixed beam room PBS nozzle and started patient treatments in November 2011.Work is on-going in two gantry treatment rooms.

6. Incorporation of beam scanning in the treatment planning: (FY 2007-2010). As described in earlier reports, we generated “beam data” with our GEANT4 Monte Carlo to enable us to use Varian’s scanning algorithm in the Eclipse treatment planning system. This gave us the opportunity to evaluate patient plans from scanned beams prior to commissioning the system.

7. Commissioning of beam scanning nozzle for gantry rooms: (FY 2008-2010). This is on-going.

8. Measurement of dose distributions in static and moving phantoms: (FY 2008-2010). Measurements in static phantoms are now routine but measurements in moving phantoms have not begun.

9. Joint Military/Civilian Proton Therapy Center telemedicine system: (FY 2006-2007). As described in earlier reports, we struggled to find a secure DOIM-approved solution that permits multipoint conferencing with shared applications over the internet. We do have a solution that allows Walter Reed physicians and physicists to remotely connect to our treatment planning system but need to improve it so there is more interaction between the staff there and at Penn. The joining of the two military hospitals caused us much delay.

Image-guided and Adaptive Radiotherapy Development

1. Pre-treatment Imaging for Volume Definition: (FY 2008-2009). Several imaging protocols are in progress (see Section III).
2. Pre-treatment Imaging for Monitoring and Quantifying Tumor and Normal Tissue Motion: (FY 2008-2009). A protocol to study this should be submitted during the summer 2009.
3. Pre-treatment Patient Set-up Using Cone-Beam CT and Other On-Board Imaging Techniques: (FY 2009-2011). The set-up room is in use and has the capability to use CBCT.
4. Cone Beam CT on the Gantry: Imaging at the Time of Treatment: (FY 2009-2011). As described above we entered into a agreement with IBA to develop a CBCT system for two gantry rooms.
5. Re-imaging/replanning during the course of treatment: (FY 2008-2011). This work has started and is on schedule. Current status can be found in Section III.
6. Development of Imaging Protocols: (FY 2007-2008). This work has started and is on schedule. Current status can be found in Section III.
7. Development of an efficient schedule system: (FY 2007-2008). This work showed great promise and was expanded as part of phase 5 of this project and will be reported in the reports for W81XWH-07-2-0121.

Progress

The work over the last year can be classified into three areas relating to progresses in: (I) Micromegas layer development, (II) spot-scanning development, and (C) protocol development.

I. Development of a Micromegas layer for proton dosimetry in 3D

The no-cost extension was approved in October 2011 and since then the Statement of Work has included the development of a Micromegas layer for proton dosimetry. The layer will provide 2D dose resolution. Multiple layers will be stacked to provide full 3D dose resolution. In addition, the layer readout is fast, so that the device will in fact have fine time resolution, and the device could be called a 4D dose monitor. Such a device would be very valuable for room commissioning and QA, and for research projects involving advanced proton delivery techniques. Because proton therapy is just now becoming widespread, there is a lack of tools designed specifically for protons, but since proton delivery equipment can modulate dose in full 3D, commissioning and QA hardware would ideally be 3D measuring devices. Currently in the clinic we use 2D technologies that were really developed for MV-scale photon therapy. This project aims to develop the 3D technology and thereby modernize the technology available for proton therapy beam measurements.

Derek Dolney is working with Professor Robert Hollebeek from the Physics Department at UPenn to develop a Micromegas-based layer for full 3D proton dosimetry. Micromegas is a technology in use at some of the large high-energy physics experiments like CERN. Bob Hollebeek is a CERN collobrator. This past year, experiments were performed both in the Physics Department using test sources and looking for cosmic ray events, and in the Department of Radiation Oncology using not only protons but also electron beams produced by the Department's therapeutic linear accelerators.

Single Channel Prototypes

The conditions for a proton monitor are similar to those for inner vertex chambers at the CERN LHC since the CERN chambers see extremely high particle rates; therefore we have selected the initial gas for testing to be 70/30 Argon CO_2. This choice is based on having extremely low radiation ageing, fast drift velocity to clear the accumulated charge, no flammable components, short pulses, and good time and spatial resolution. These gases have been well studied and their properties are well known. The next figure for example shows the drift velocity at 0.75 kV/cm to be about 2cm per micro second. [Yuan-Hann Chang et al. NIM A311 (1992) 490-497]

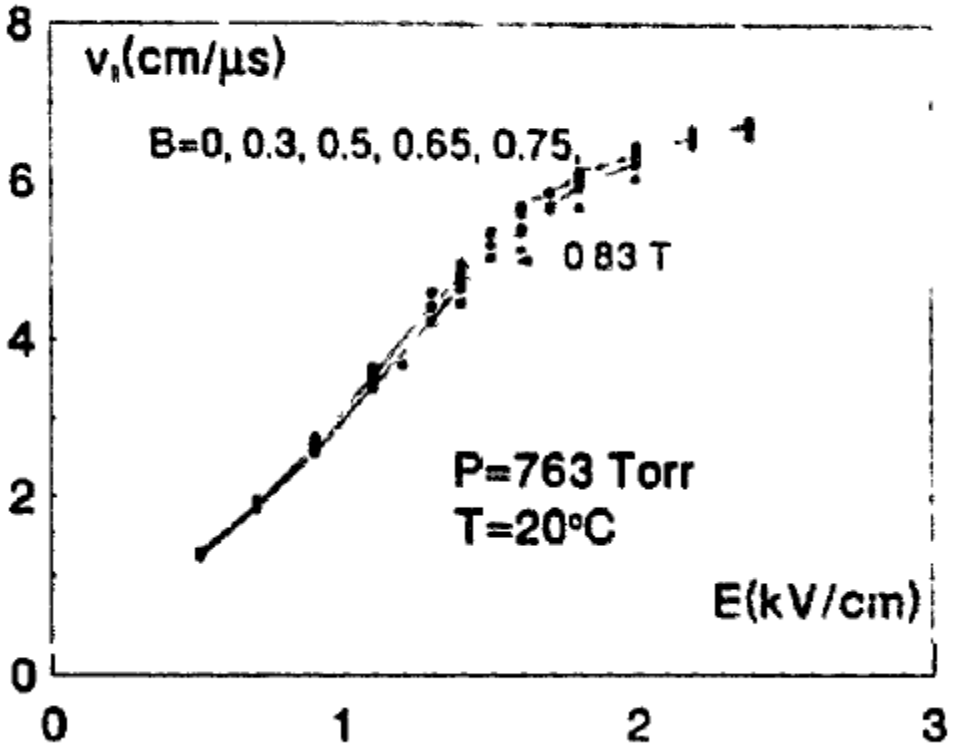

We completed the construction of a test system with gas supplies, high voltage systems, low noise preamps, oscilloscope, radiation sources, a pair of scintillators for using cosmic rays, calibration signals, and coincidence electronics for cosmic ray triggers. The test system also has a multi-channel analyzer and computer system for taking pulse spectra. The figure which follows shows a single pulse from a Sr90 calibration source.

Chamber prototypes are constructed from modular planes and can be easily modified or combined together. The figure shows a two gap prototype which was constructed from a pair of

single gap systems. A modified version of this chamber will be used in electron and proton beam tests in the next quarter.

Operation in the proton and electron beams will require an adjustable gain in the gap of about 1 to 10. While gas gains of 10^4 to 10^5 are possible in these systems, since we are detecting relatively large currents rather than individual pulses, the required gain is much lower.
During Q1 2012, Derek and Bob Hollebeek (Physics Department) continue to investigate various construction techniques for ionization and Micromegas chambers. We have two designs which can be used to implement a wide gap (5mm) or small gap (1.67mm) ionization chamber using either a wire mesh stretched over a PVC frame or braised to a copper ring. We have also developed a technique to produce a laminate of an insulating mesh and the wire mesh which could be used to produce chambers with a 250 micron gap. Example single-channel prototypes are shown in the next figures.

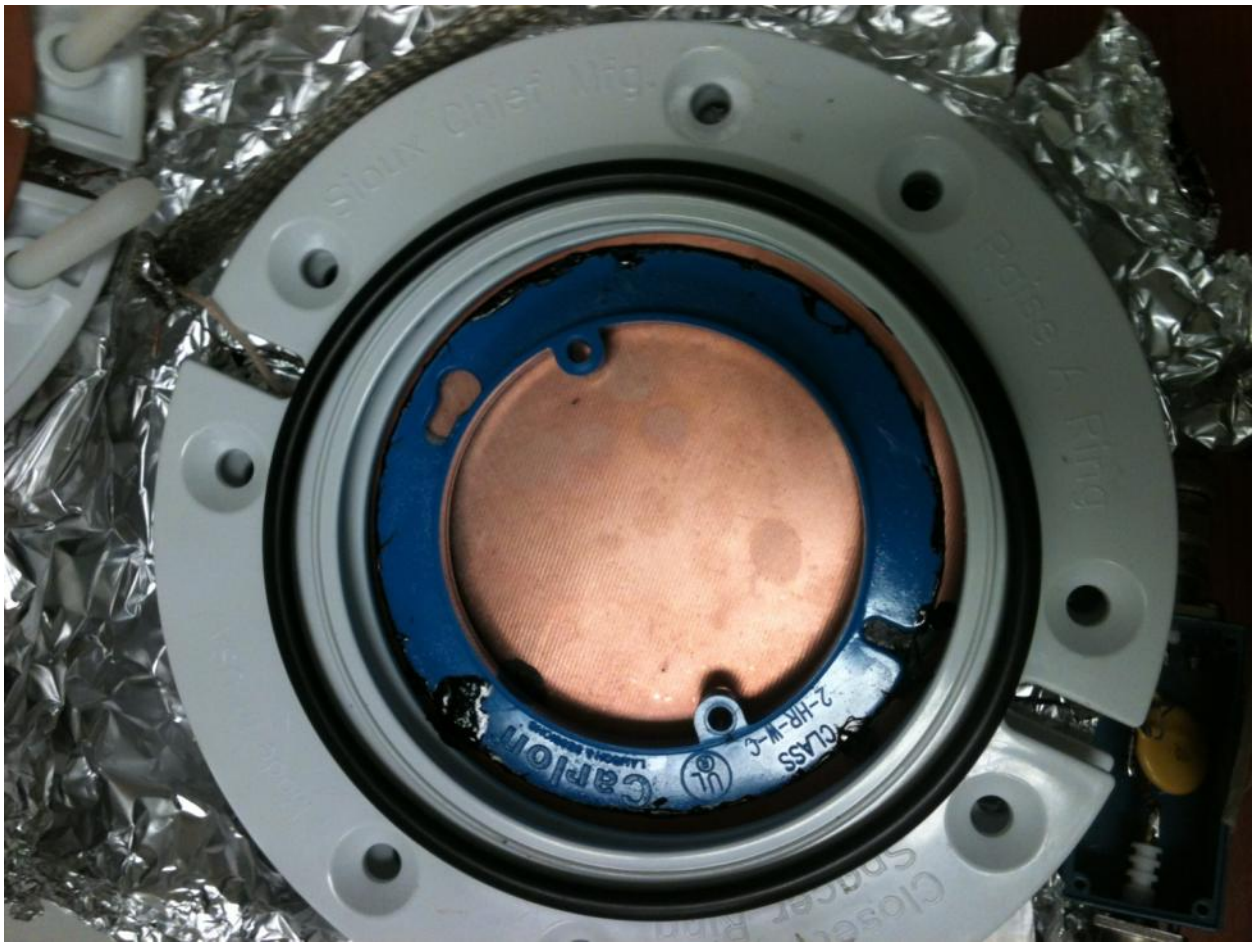
Carlon
CLASS
2-HR-W-C

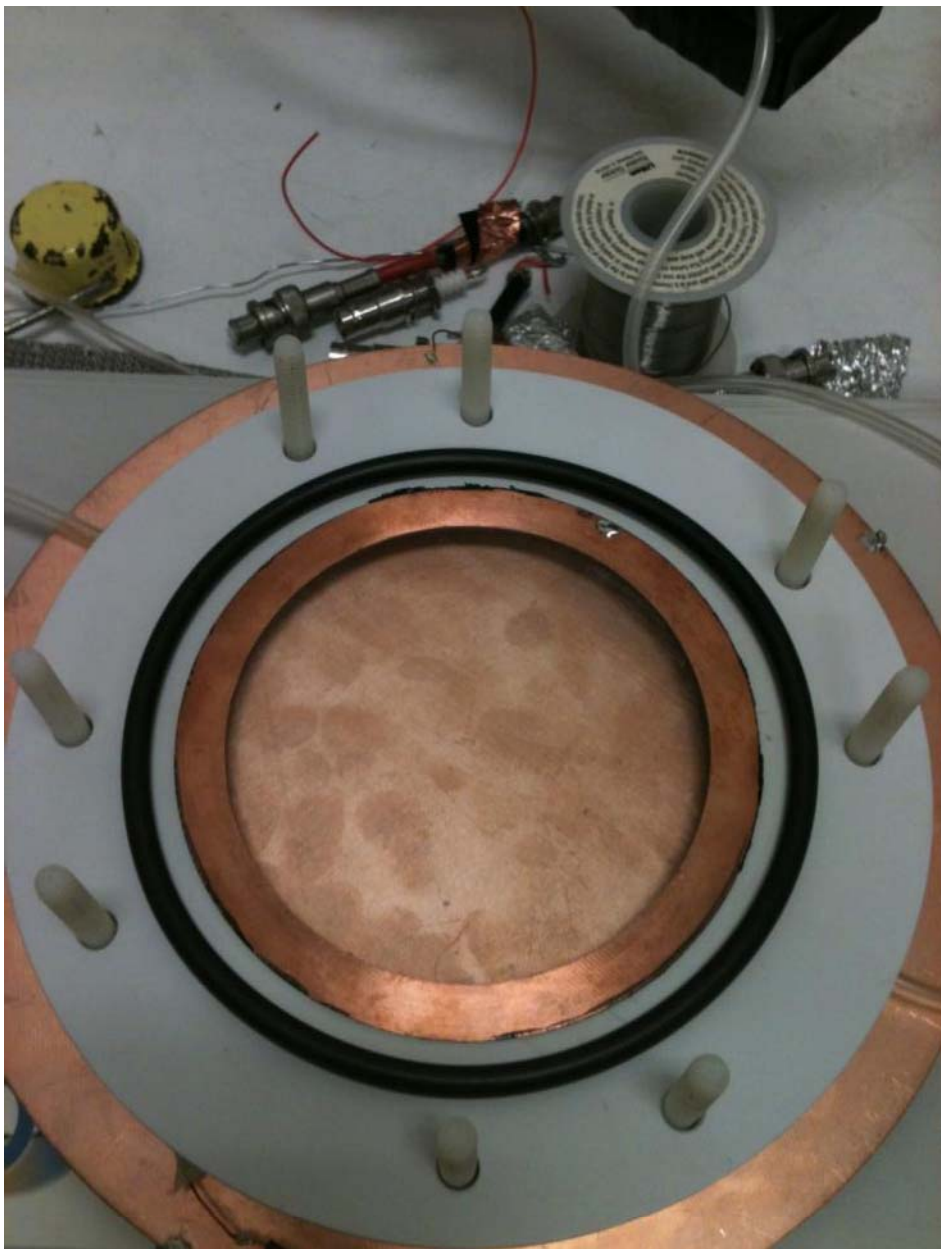

When under voltage, electrostatic forces eliminate any gap between the insulating mesh and the cathode surface (seen as a shadow in the next figure).

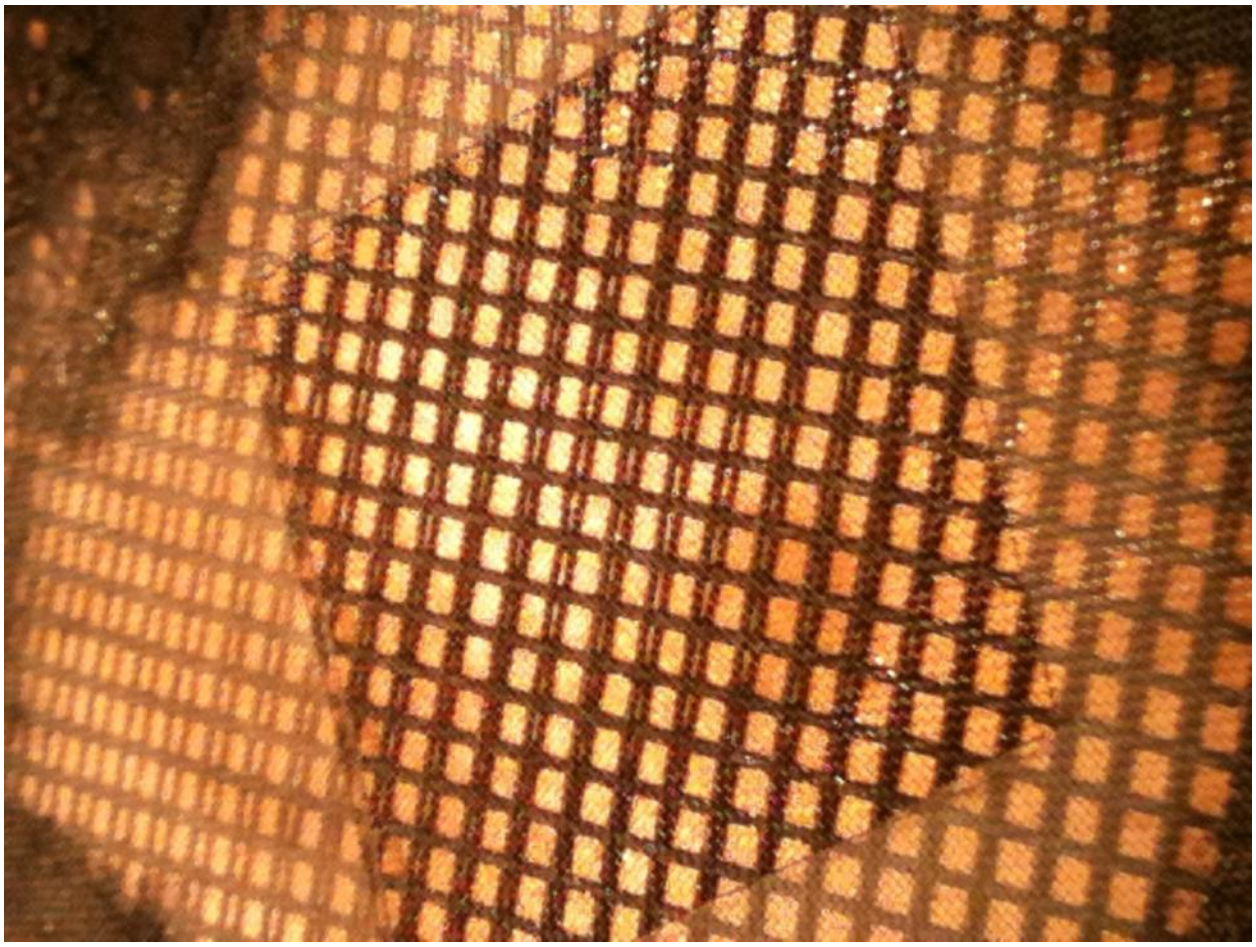

In the large gap chambers, the voltage on the wire mesh is positive and electrons drift toward the wires.
In a Mmicromegas hundred micron scale gap however the mesh is at a negative voltage. Electrons drift toward the mesh due to a slightly higher drift potential then pass through the mesh and are amplified below it. This has numerous advantages for high rate environments since large numbers of positive ions are confined to the region below the mesh.
We have performed some more measurements with one of the single-gap Micromegas prototypes in proton room #2 using pencil-beam delivery. The detector was placed downstream of solid water. We hoped to measure a Bragg curve this way to demonstrate that the detector does not quench in the peak. The next figure shows the gain curve measured with prototype #2 in the proton Treatment Room #2. A single pencil beam of maximum energy (226.7 MeV) is delivered through the center of the prototype. The bias voltage is the potential of the top plate that defines the drift region. The mesh is held at 80% of the top plate (voltage divider). We achieve gains of 30 or so with this prototype. The bias voltage is limited by arcing inside the prototype. The amplification gap is defined by a 1.7 mm thick spacer ring of diameter 10 cm. At high voltage the mesh deflects towards the anode and eventually arcs. We are working on better ways to maintain uniform gaps of various thicknesses. One solution is to use a woven fiberglass or PVC screen. Bob has successfully laminated the screen to a copper cathode, but the gap is fixed to be the thickness of the screen (1 mm). We have assembled a thicker gap using nylon washers as spacers. The washers are also 1.7 mm gap, but in this case they are arranged in a grid. This prevents the mesh from deflecting across such a wide area and the

performance is somewhat improved. Of course, the CERN parts are laminated with Kapton standoffs spaced every 5 mm between the mesh and cathode which maintain a uniform gap, but we need prototypes of different thicknesses to choose the gap dimensions first so we continue to try to develop in-house solutions.

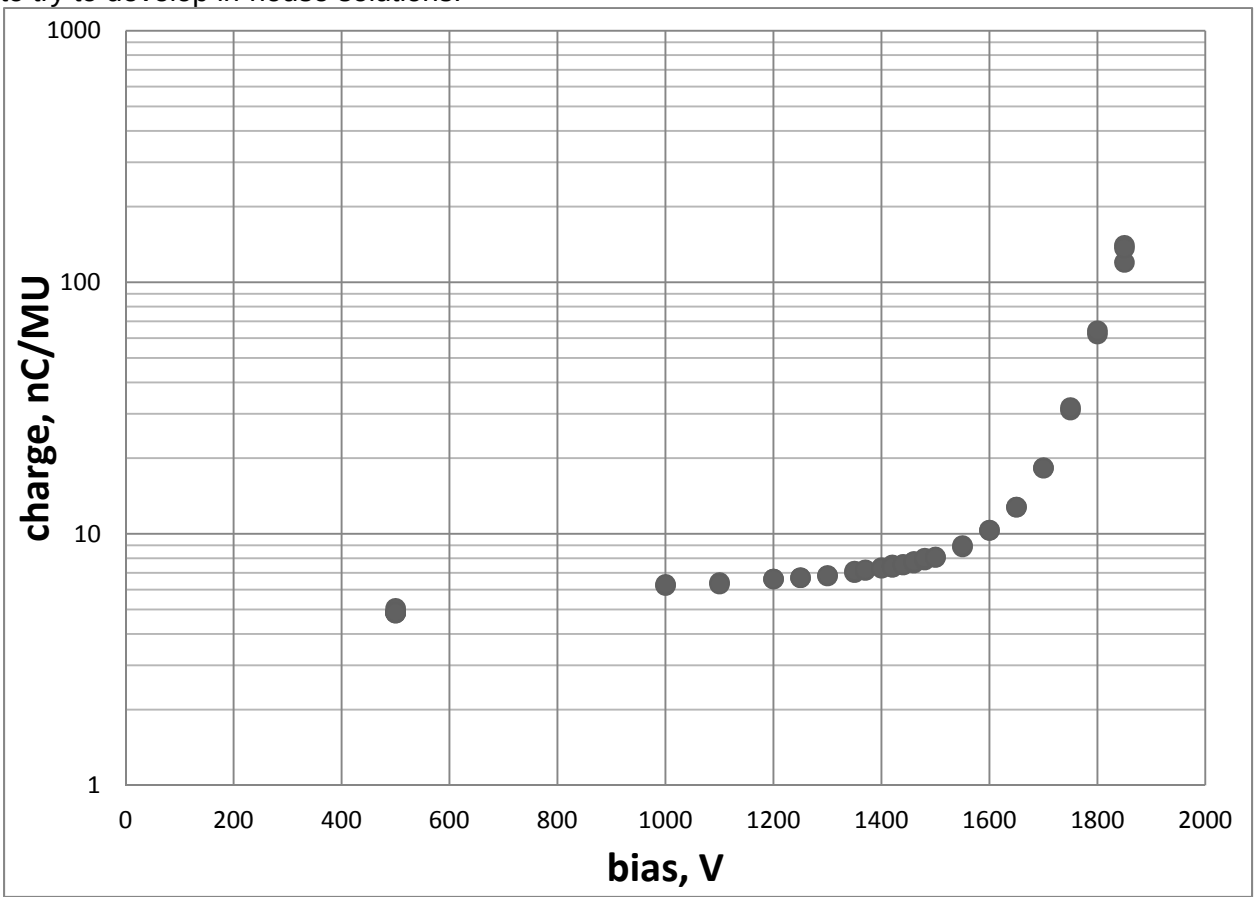

The next figure shows the gain measured with prototype #2 for different beam currents. The current is that at nozzle exit, or equivalently, the current passing through the prototype itself. At low current, we are collecting most of the charge and do well, but already at 2 nA the collection efficiency is lost probably due to recombination. Since our goal is to resolve the dose rates from the peak in the center of the pencil beam out to the 1 or 2% level in the penumbra, and we will not have an independent current measurement of the beam current at the measurement points, a key outcome of this phase of research is going to be to find a set of dimensions and operating potentials that provide stable gain over a wide range of beam currents. The next figure suggests that we should keep the field strength in the amplification gap below 1500V / 1.7 mm or about 9 kV/cm.

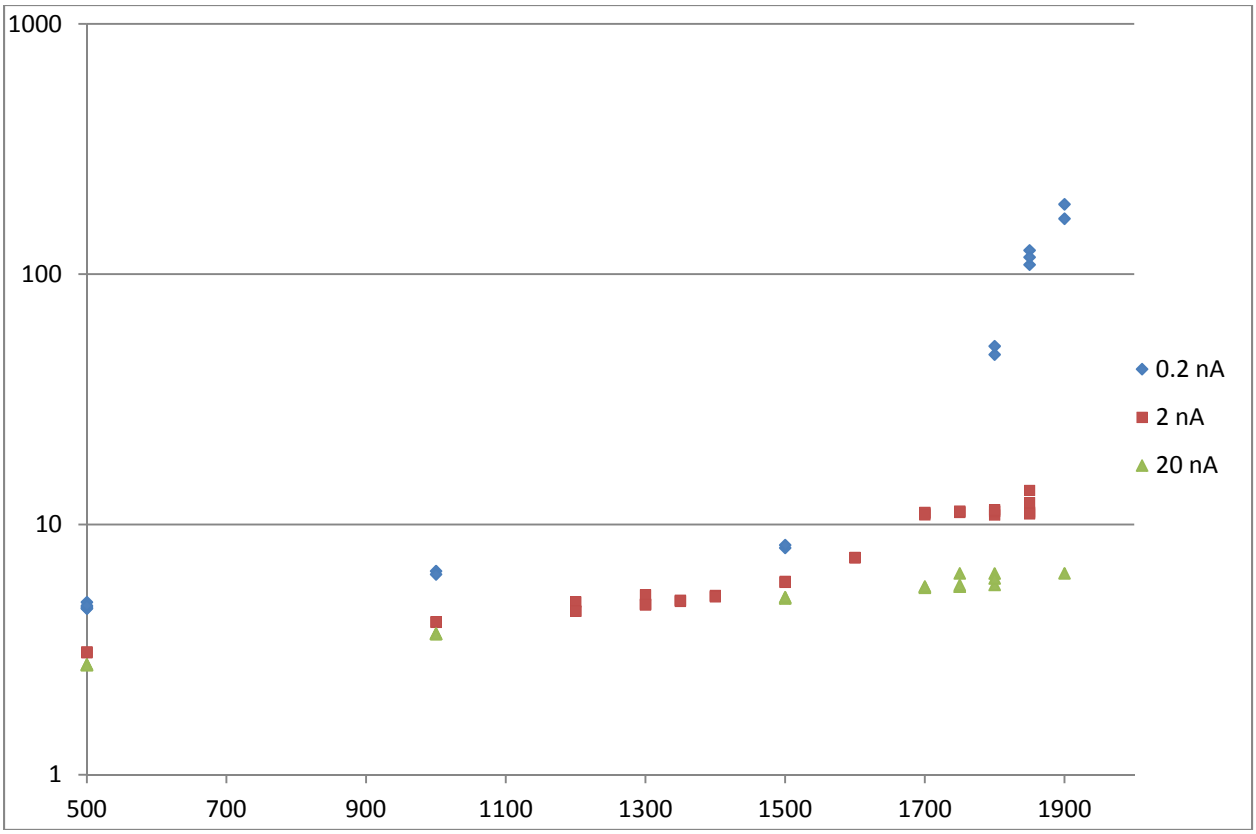

Computer Simulations of Micromegas Chambers

We are using computer simulations for guidance in making design choices for the Micromegas chambers. We have implemented the chamber geometry in Geant4 Monte Carlo simulation and can add Micromegas chambers to the existing IBA nozzle simulation code already developed at UPenn: the double-scattering and uniform-scanning simulations including the MLC implemented by Chris Ainsley, and the pencil-beam delivery implemented by Derek Dolney. The next figure shows a Geant4 simulation of the chamber geometry and fields.

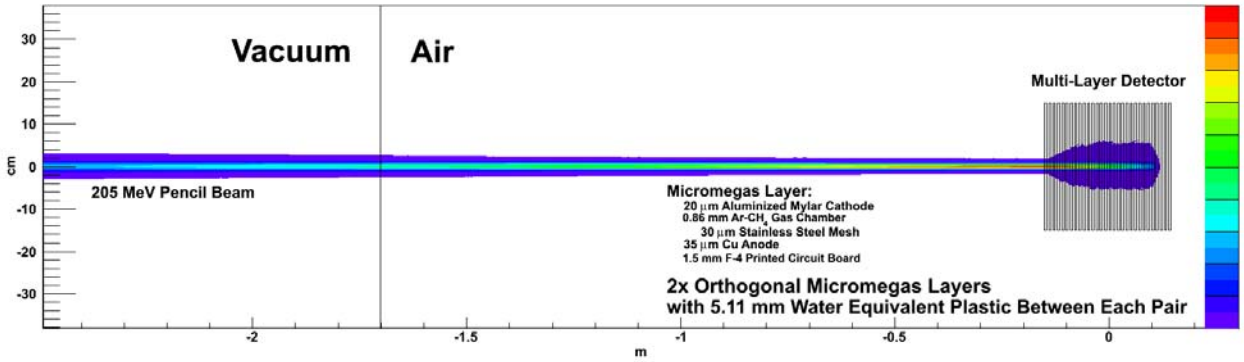

We are also using the Garfield software to simulate the electromagnetic field in the chamber. An example Garfield output is shown next.

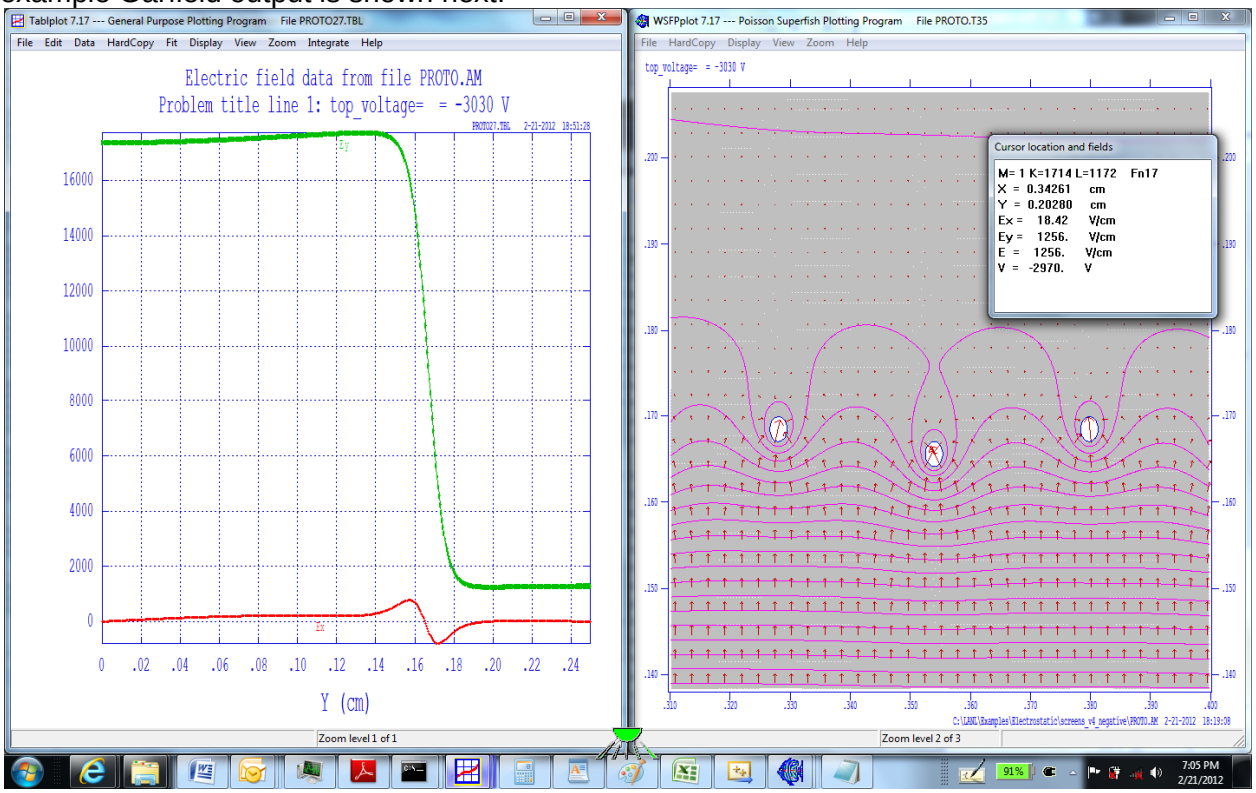

We are using these field simulations to guide our choices of operating potentials, gap thicknesses, and to help understand some of our measured results. We have not chosen materials for tissue-equivalence because it will depend on the final dimensions, mostly the gap size. Note in the plot on the right that the fields above the wire mesh are bent in such a way as to produce a focusing effect toward the hole for electrons travelling out of the upper drift region. We have implemented the copper sheets, printed circuit layers, and gas in Geant4 simulations and can simulate the three modalities of proton delivery to the Micromegas geometry using the existing simulation code including the proton MLC. Some simulation results of SOBP and pristine Bragg peaks deliveries are compared with data measured by a Micromegas prototype below.

Multi Strip Prototype

To test the position resolution of these devices in electron and proton beams, we have constructed a prototype with a readout plane which is divided into 8 strips and a left and right guard region. The plane is divided in half so there is an upper and lower half making 20 channels total. The first 20 channel prototype was produced in Q1 2012 and is shown in the next picture.

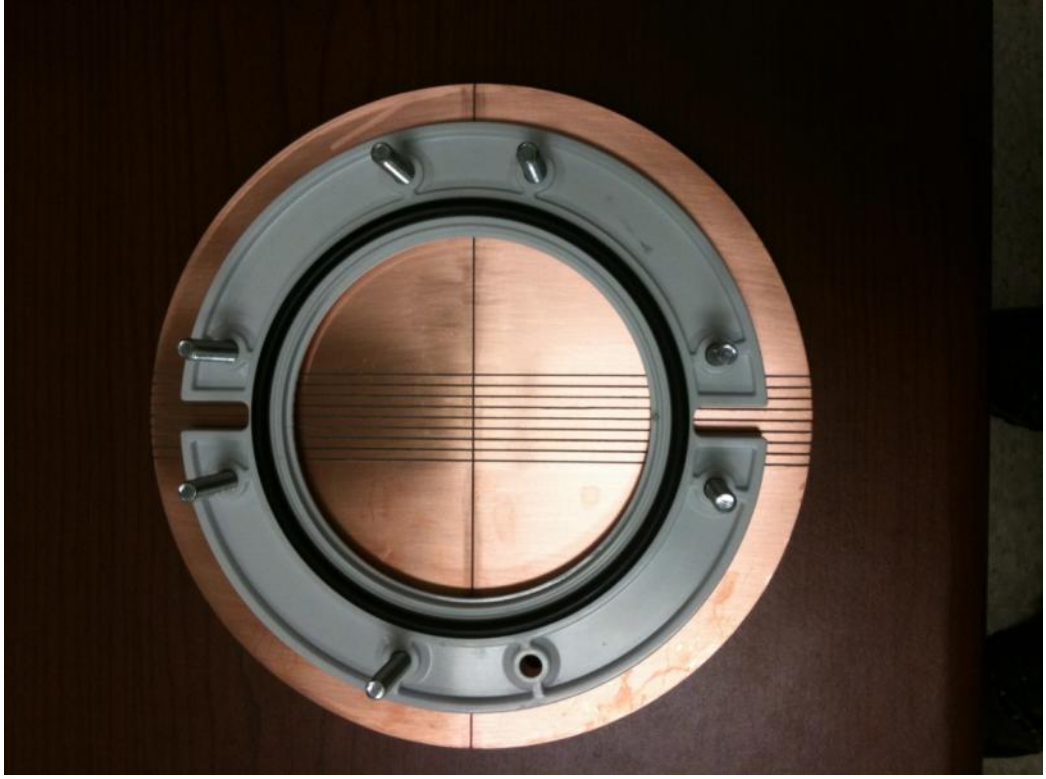

Readout Chain

To readout the multiple channels of layer, we have designed a readout chain consisting of pre-amplifier boards, a readout DAQ, and have written some PC software to control the data acquisition.

The preamp and readout for the strip detector and the pad detector are the same. The design was finished in Q1 and the first two boards have been assembled and will be tested in Q2.

The readout system uses a custom design proton monitor preamp board (designed at Penn) together with a commercially available readout (DI-720).

The DI-720 has 14-bit resolution and 150-200kHz waveform recording capability. It communicates with a PC through an Ethernet link. Each device has 16 differential analog inputs . We require 10 differential inputs for the Proton Monitor in the strip layout. All channels support a measurement range of 1.25 to 10V full scale and gain factors of 1, 2, 4, and 8 are programmable per channel.

Two boards of the custom design 10 channel Proton Monitor Preamp Board have been produced and will be tested in Q2. The channels have a dual gain configuration which is controlled by outputs from the DI-720. The specifications are:

Hi-gain mode: 20mV/nA design. (16.6mV/nA measured in spice simulation.)
14bit ADC: 16384 counts
Vdc Range = 10V (+-5V)
Least count (SPICE) = 10/16384 = 0.610mV/cnt
Resolution = 36.8 pA/cnt.

Actual Gain may be higher due to differences in simulation of the switch and the real switch.

Lo-gain mode: 500mV/uA design. (488mV/uA measured in spice simulation)
14-bit ADC: 16384 counts
Vdc Range = 10V (+-5V)
Least count (SPICE) = 10/16384 = 0.610mV/cnt
Resolution = 1.25nA/cnt

The board layout is shown in the following figure.

PROTON MONITOR PREAMP BOARD LAYOUT

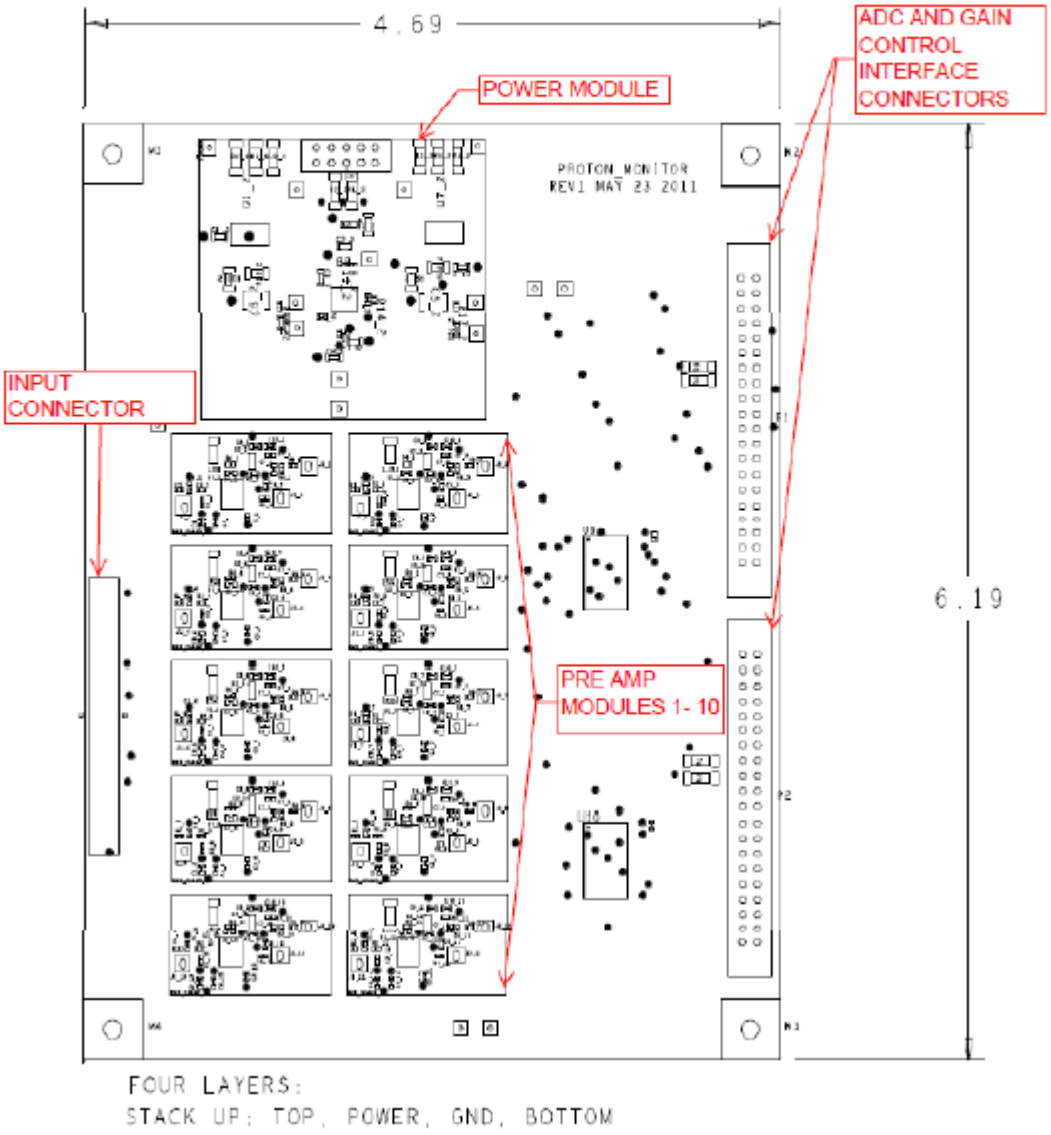

This dual gain system uses one opamp with two feedback loops per channel, one permanently wired, and the other switched on by a logic level. The gain can be set individually using digital I/O bits available on the DI-720 A/D convertor board. This provides dual gains for each channel, that feed directly into the multiplexed A/D inputs, switches and buffers for additional digital I/O gain control. This system provided flexibility for adjusting the gain across the plane.
While lots of automatic techniques are possible, the simplest (therefore fastest) way to automatically adjust the gain would be to have a monitoring program look at the data as it's coming back and go to high gain if the output goes below 1/20 of the full scale range. The

output would stay fixed unless it went above its 10X upper window limit ~1/10 of the coarse scale reading. This kind of switching could accommodate wide variations in dose across a treatment field. A picture of one of the dual power supplies boards is shown here.

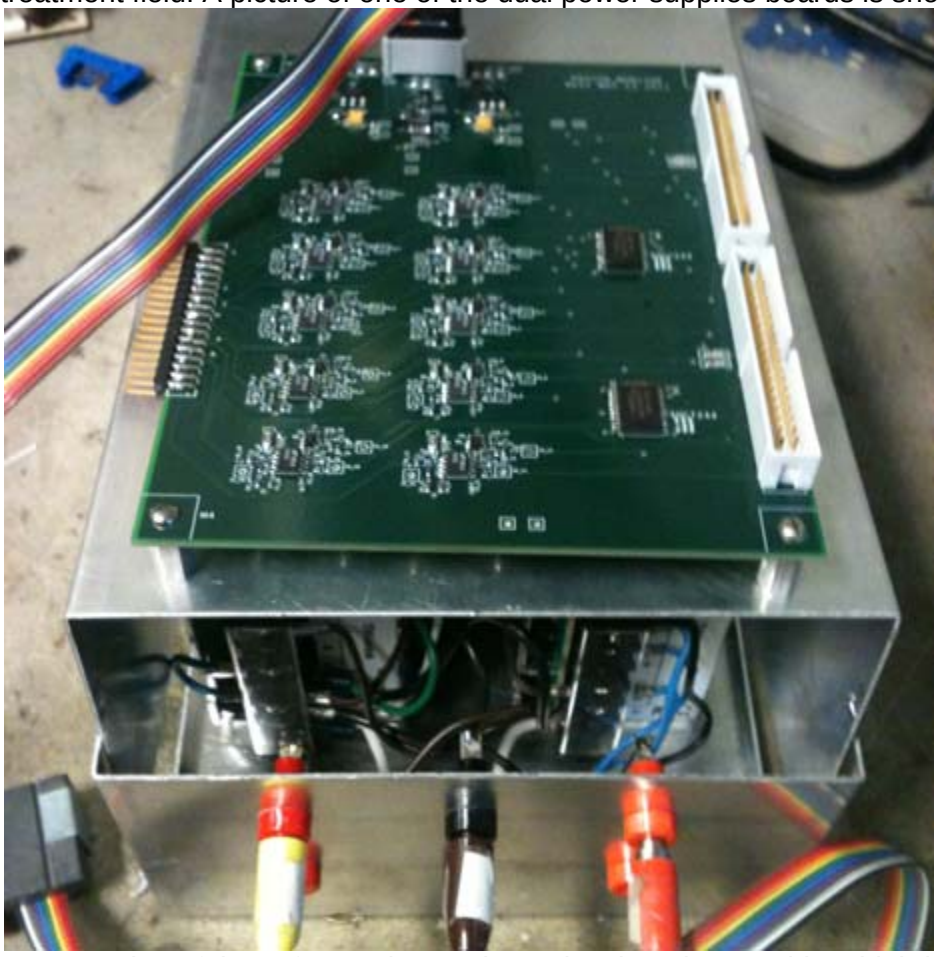

A screenshot of the software that we have developed to provide a high-level user interface to control the DAQ and handle the multi-channel data from the DAQ is shown next. The software was developed mostly by a physics student, Gaurov Shukla. The software records multiple channels and also allows to switch the individual gains for the channels. A plot of 10 data channels is displayed on the computer screen in real time. The acquired data is written to a file that can be re-opened, manipulated off-line, and saved as comma-separated values for work in Excel, gnuplot, or elsewhere.

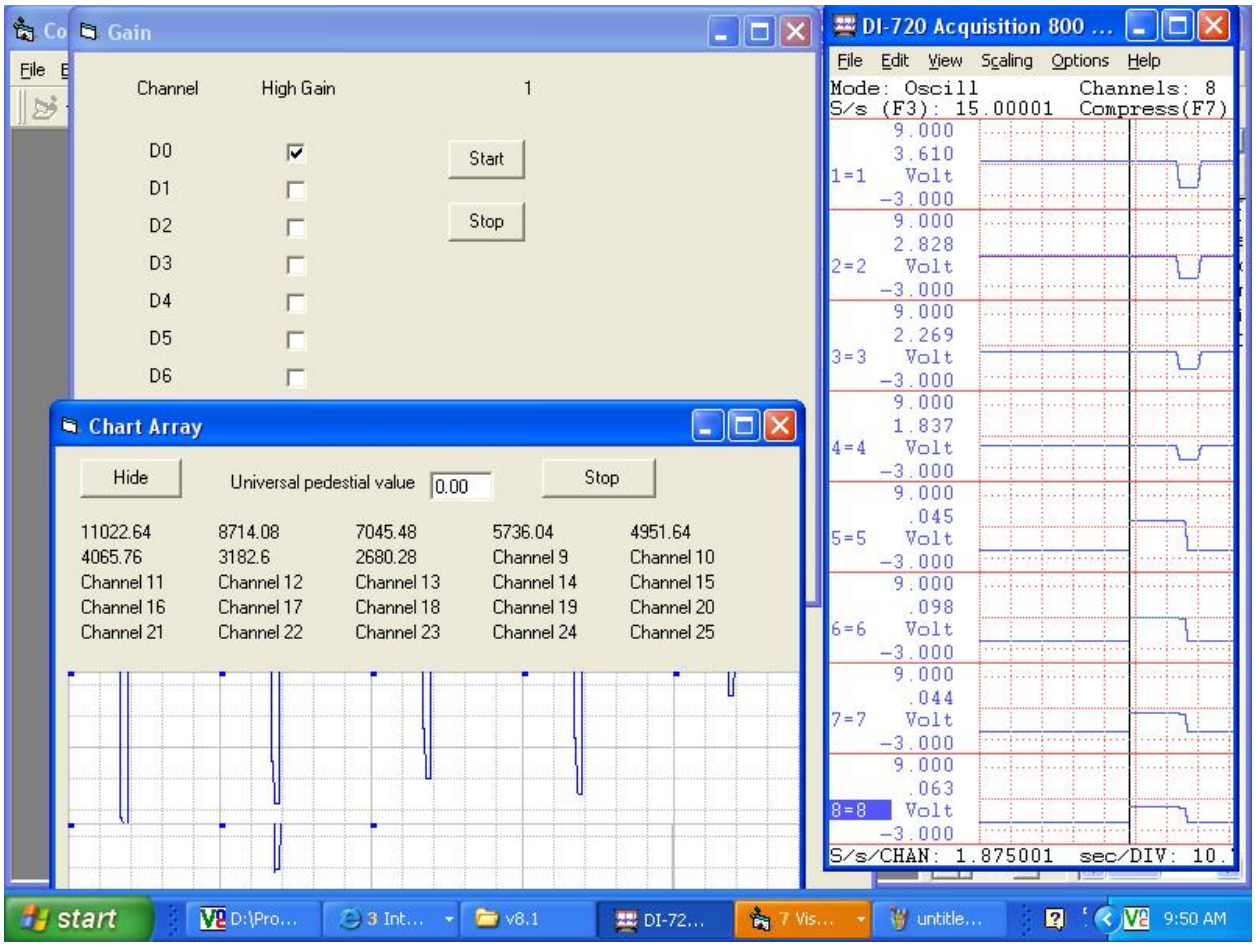

CERN Pilot Device

We have obtained from CERN a 5-channel pilot Micromegas device. During Q1 2012, we prepared the mechanical design for this first pilot Micromegas chamber produced at CERN using the BULK Micromegas technique. The gap region is constructed from PEEK insulators and also provides gas inlets and outlets, gas seals, and provision for a spring connection to the mesh plane.

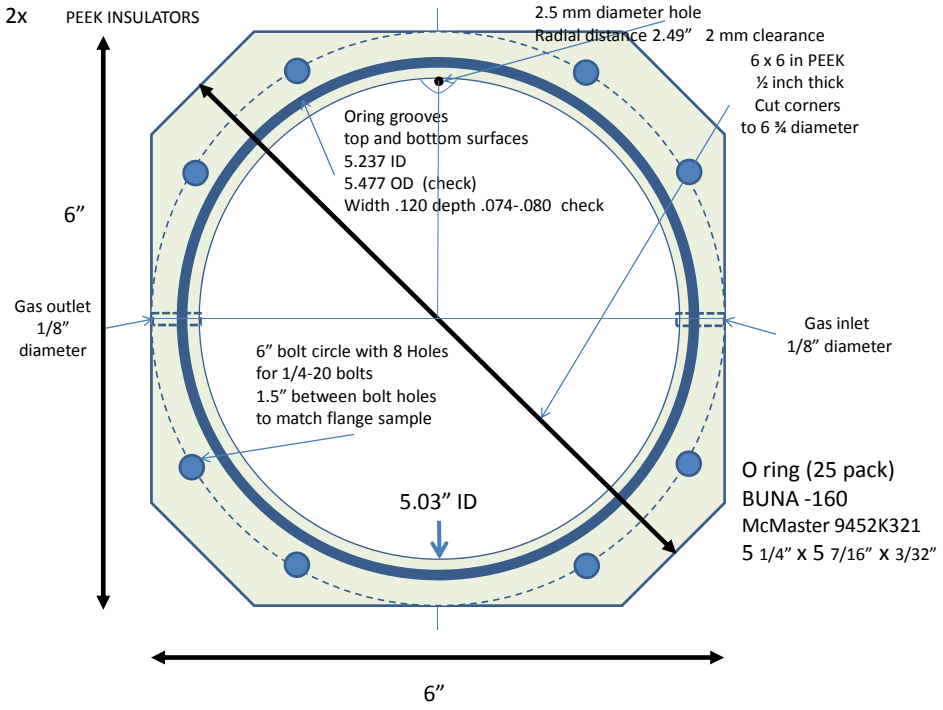
2x
PEEK INSULATORS
2.5 mm diameter hole
Radial distance 2.49”
2 mm clearance
6 x 6 in PEEK
½ inch thick
Cut corners
to 6 ¾ diameter
Oring grooves
top and bottom surfaces
5.237 ID
5.477 OD (check)
Width .120 depth .074-.080 check
6”
Gas outlet
1/8”
diameter
Gas inlet
1/8” diameter
6” bolt circle with 8 Holes
for 1/4-20 bolts
1.5” between bolt holes
to match flange sample
5.03” ID
O ring (25 pack)
BUNA -160
McMaster 9452K321
5 1/4” x 5 7/16” x 3/32”
6”

The next picture shows the pilot device assembled with the insulator ring visible. The cathode layer is divided into a central region and 4 surrounding regions for the beam test. The gap size is 300 microns. The mesh is supported above the cathode by the small support posts which can be seen distributed on the surface. The mesh HV feed is on the right.

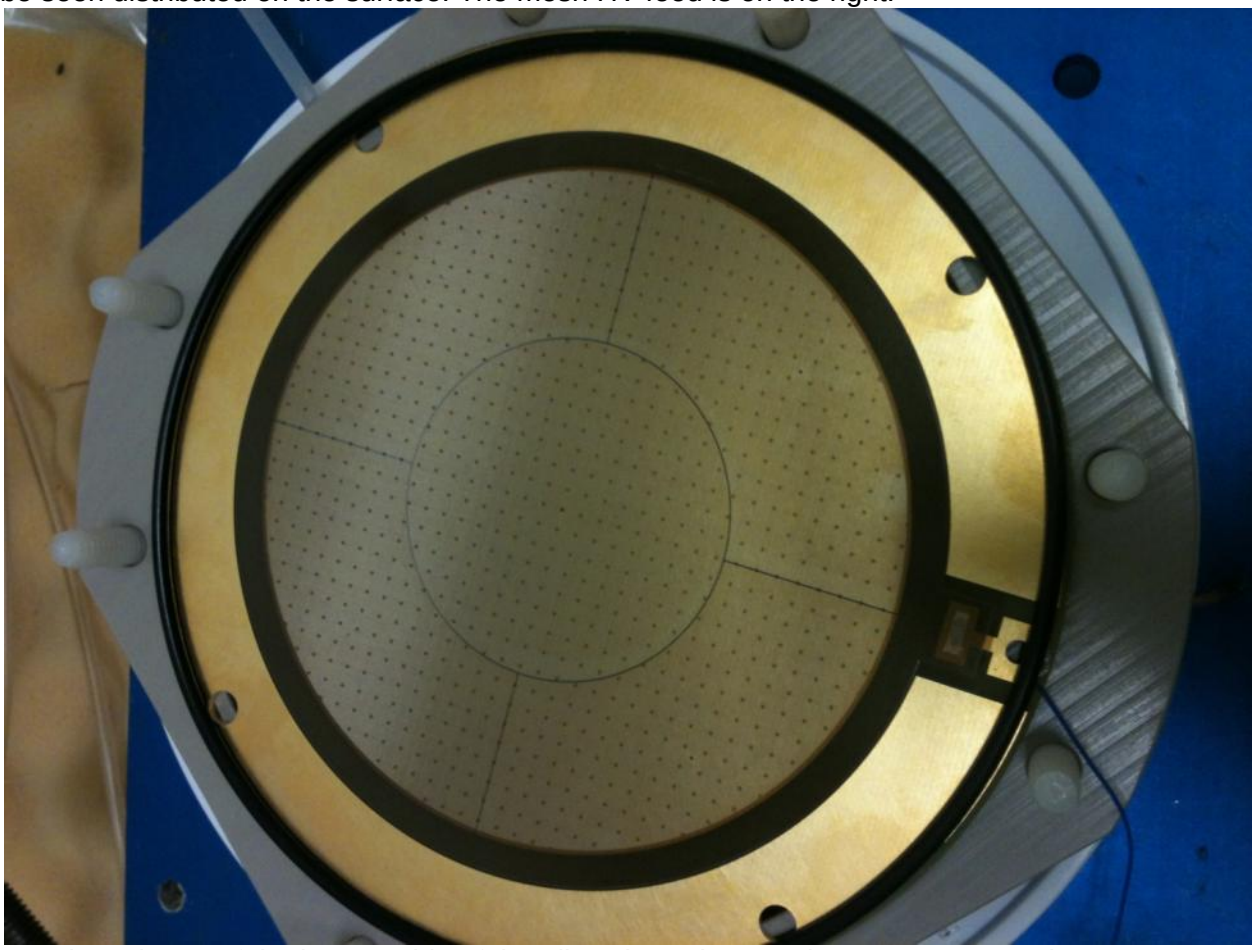

Next is a picture of the bottom side of the pilot where the 5 regions are connected to output cables leading to the preamps.

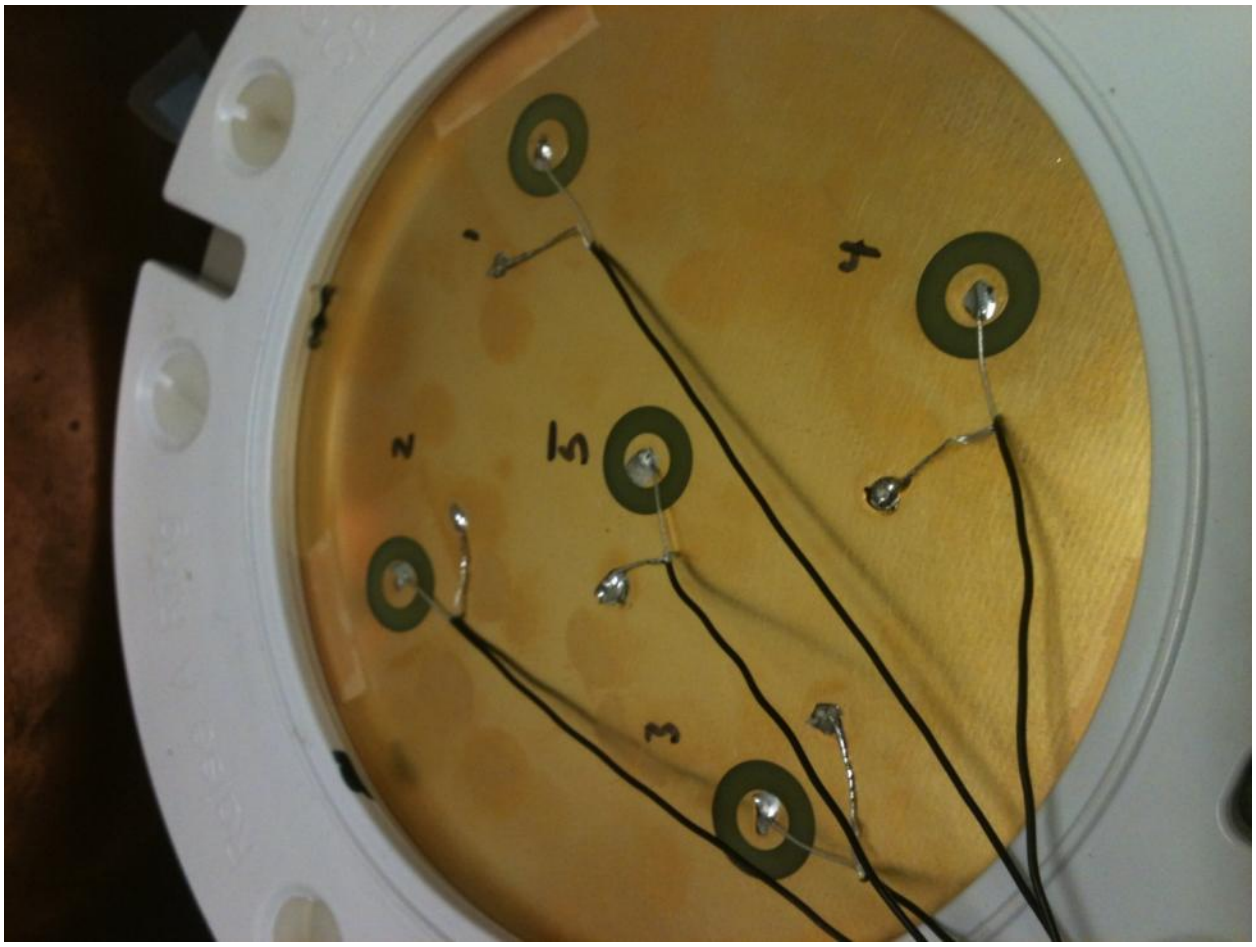

The pilot device has been tested in 70/30 Argon Co2 low gain gas using an Fe55 source which is embedded within the chamber. Below is the resulting calibration curve. The calibration was

stable to less than ½% overnight without correcting for changes in atmospheric pressure.

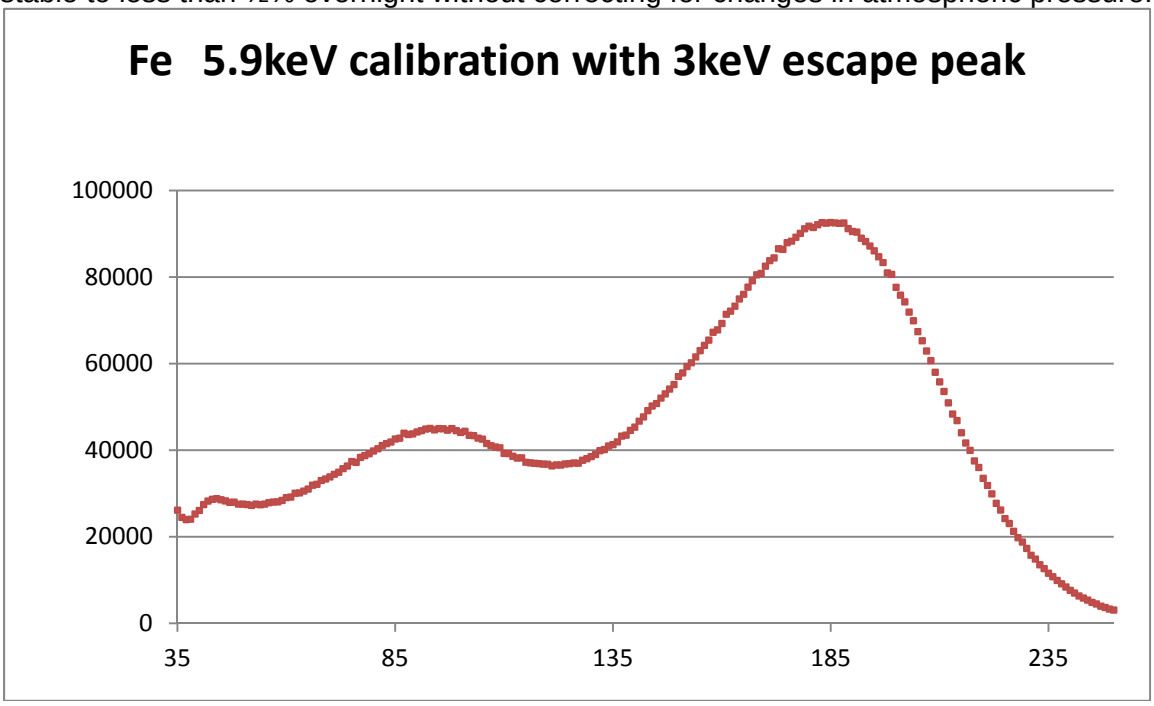

The F355 source provides an absolute calibration of the entire chain of electronics which includes the chamber gain, the preamp gain and the amplifier gain. The following figure shows a separate calibration of the preamp/amp using an injected charge pulse which allows us to extract the chamber gain.

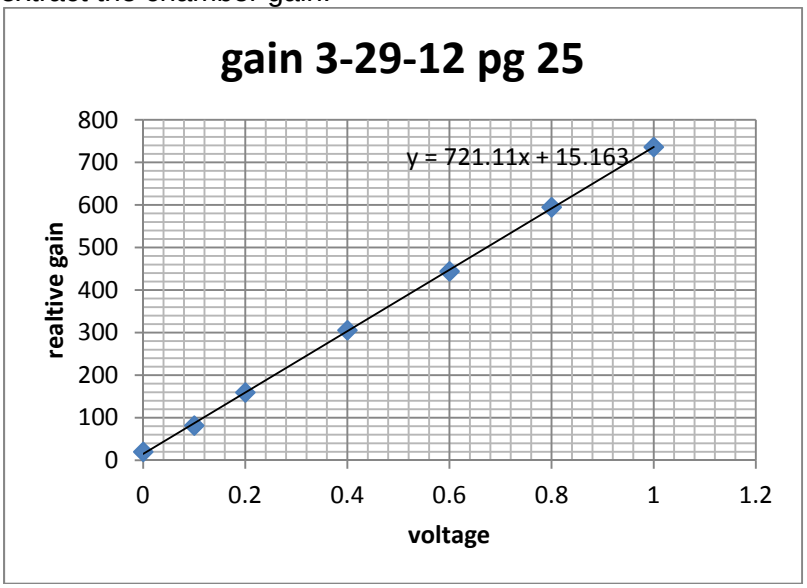

Next is the resulting gain curve as a function of mesh voltage for a fixed drift voltage of 710 volts.

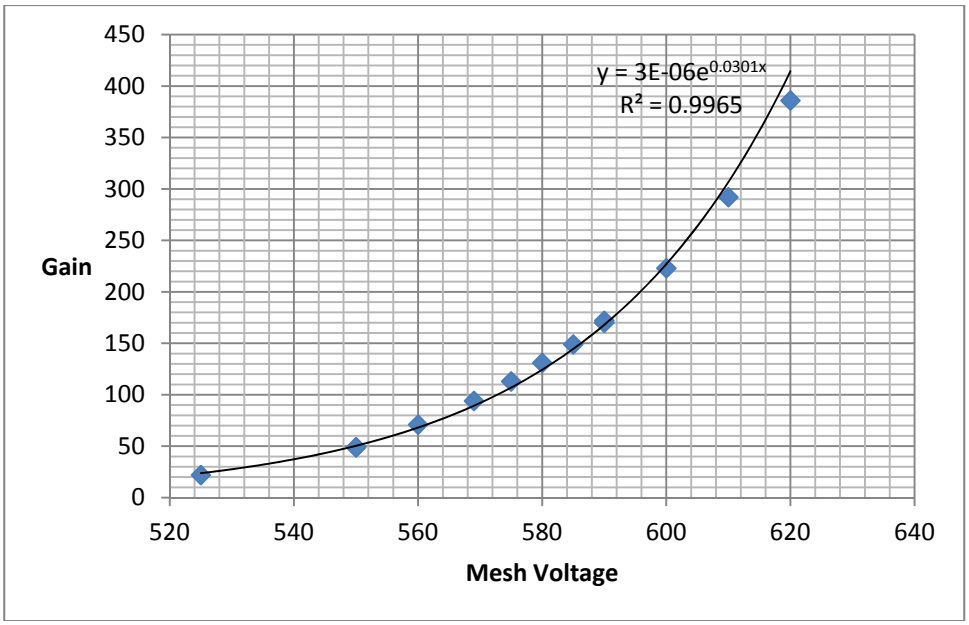

The next three figures show individual pulses from the chamber.

Figure: cosmic ray trigger (cyan), preamp output (green) and amplifier output (magenta)

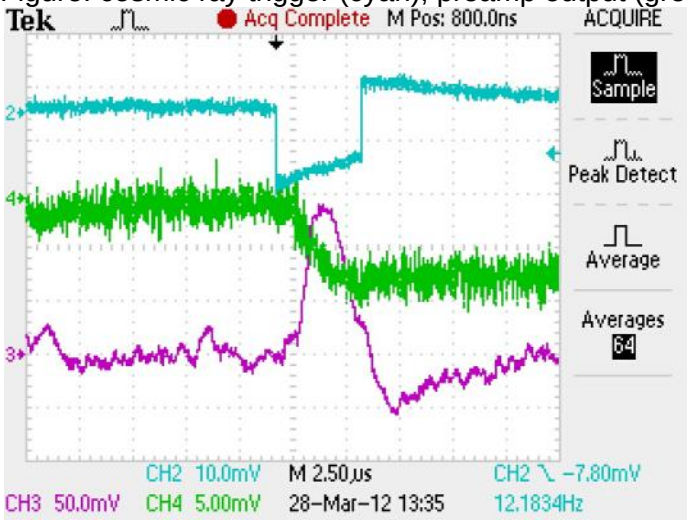

Figure: single pulse from the source

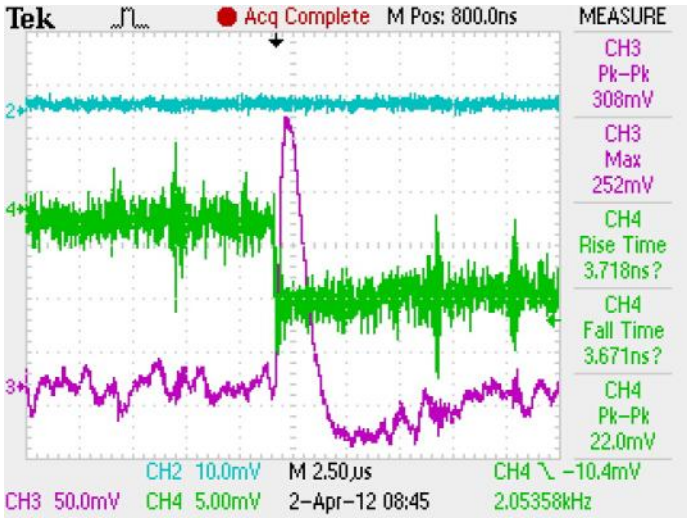

Figure: Pulse average from the source

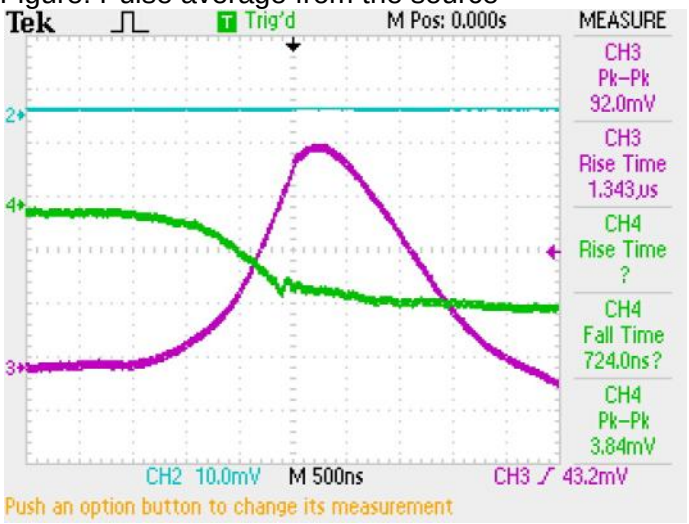

We have successfully measured the distal end of an SOBP with the Micromegas pilot device. Our experimental setup is shown in the next few photographs. First are the two chambers, to be irradiated from above. The top chamber is the multi-strip Micromegas prototype. The gap is large so that chamber has no gain, i.e. is running in ionization mode. The 5-channel Micromegas pilot device is inside the copper shielding box. Gas flows through both chambers and both are sharing the same high voltage feed.

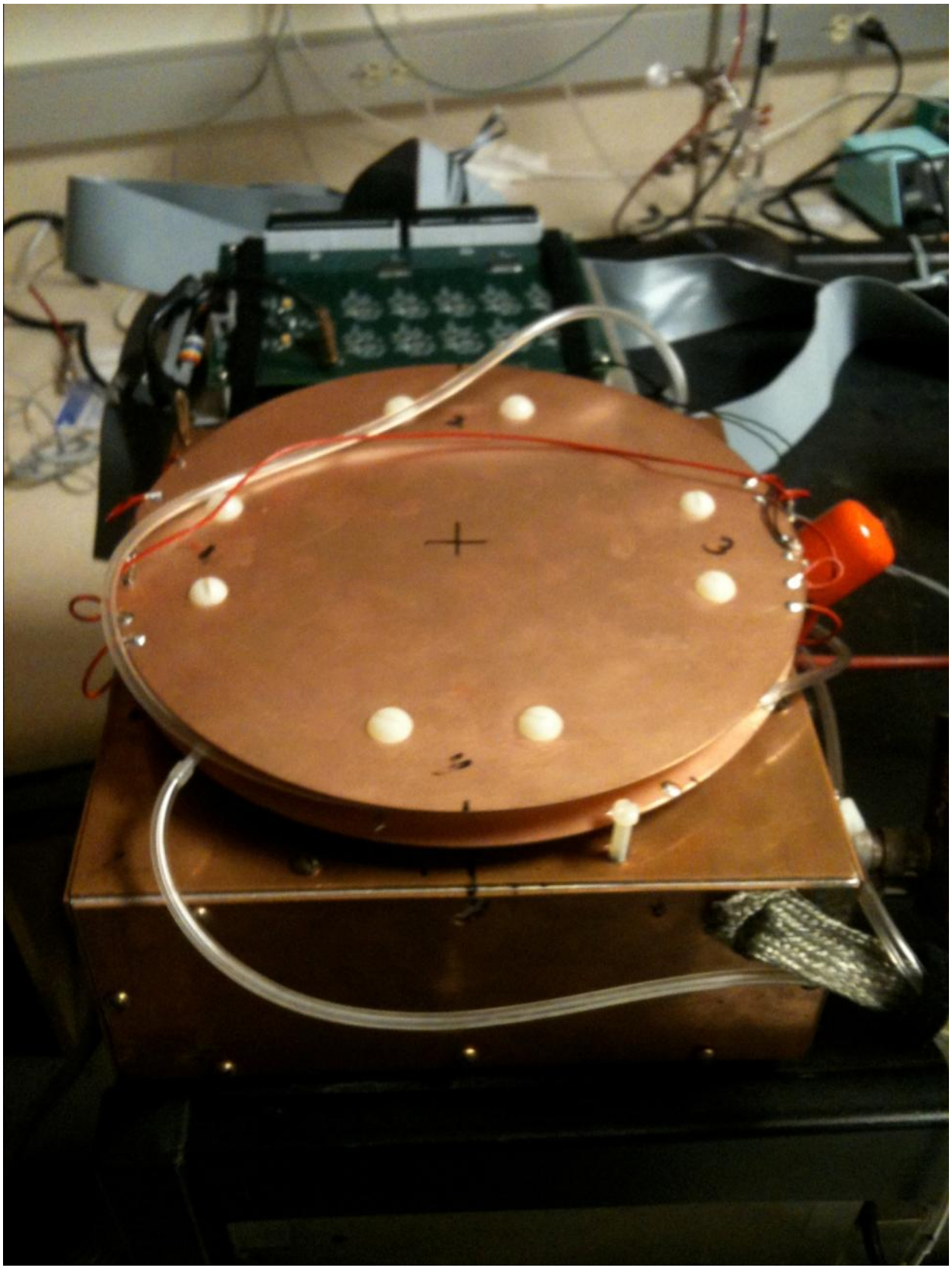

This is the experiment setup in the proton room. We are using the MLC to collimate to a very small 5 mm x 5 mm field in order to simulate the flux that the 5 mm x 5 mm voxels of the pixellated CERN prototype will see.

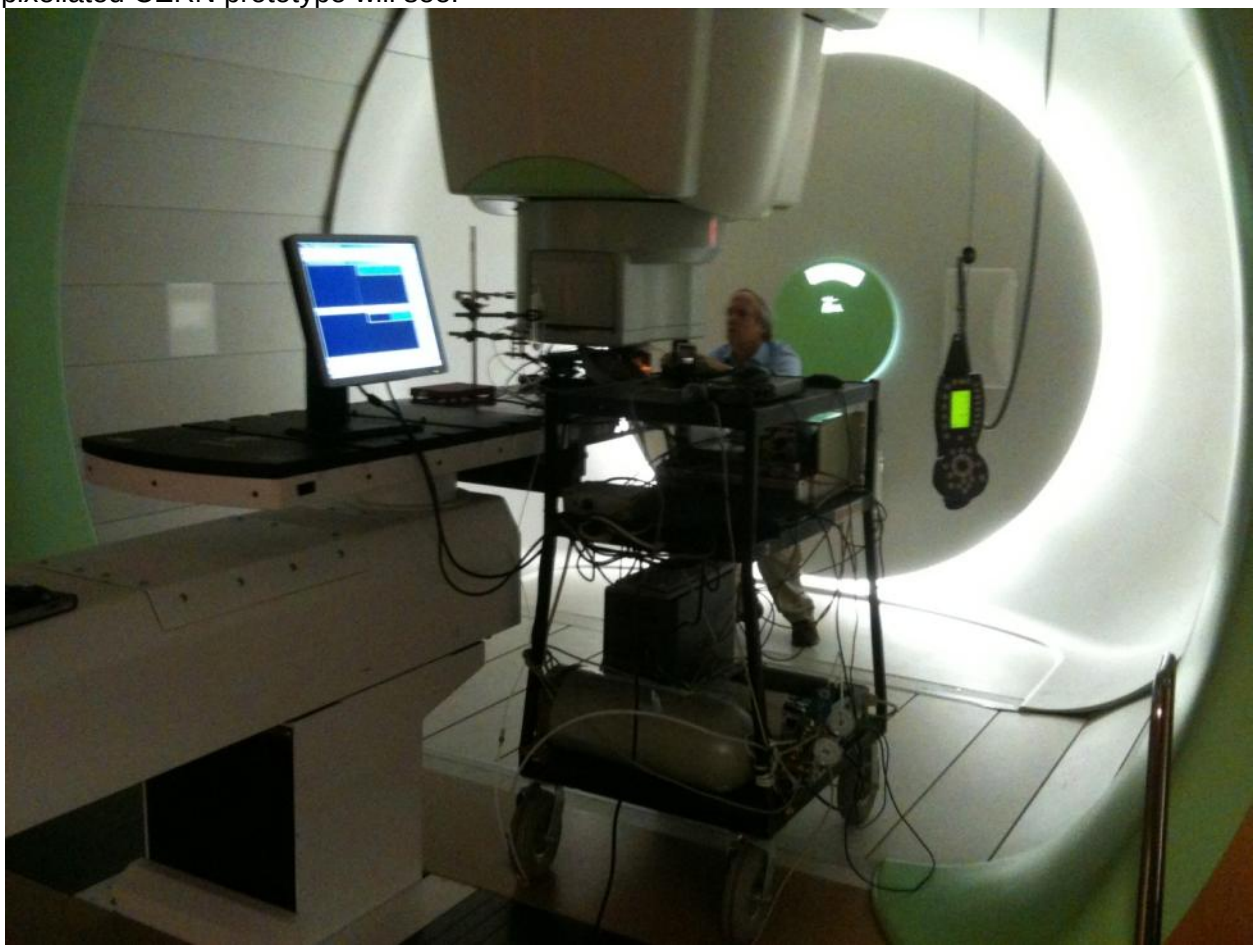

Below you can see the chambers centered just downstream of the MLC.

For the SOBP measurement, the couch was lowered, a tank made of lexan was placed on top of the chambers, downstream of the MLC, and filled with water, and an R17.5 M10 SOBP was delivered to the Micromegas chamber. A drain tube was used to flow water out of the tank continuously while the beam was on and data was collected. In this way, we hoped to collect an entire SOBP quickly without having to reenter the room and adjust water depth or solid water stack. The water tank worked well, but we did not have enough time to collect the entire SOBP yet. The tank starts full, so we got the distal falloff and some of the plateau of the R175M10. The next figure shows the data that we collected. You can see the tuning pulses, and some data where we checked that our gain settings were not saturating in the dose rate within the SOBP. Then the tank was filled and the beam restarted to gather the SOBP data.

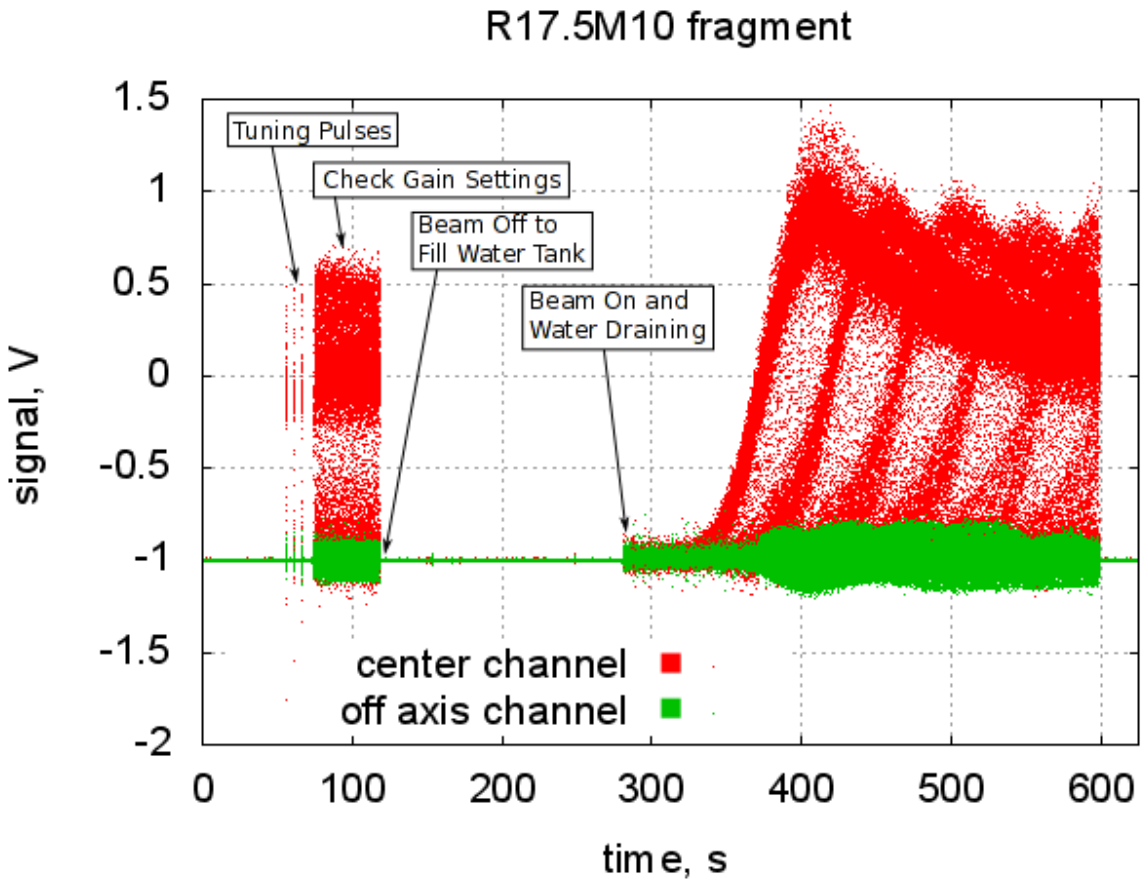

This is a double-scattering delivery, using a range modulator wheel. Each segment of the modulator wheel delivers a different pristine Bragg peak, and you can see the pristine peaks in the SOBP data. The dose at any given depth should be the sum of the dose of all the pristine peaks. We have performed the sum over each wheel rotation. That is shown as the black curve on the next plot. The depth was obtained by recording the water level as a function of time. By adding the water-equivalent thickness of the copper and printed circuit layers above the Micromegas pilot, we obtain a range measurement for this beam: 17.2 cm.

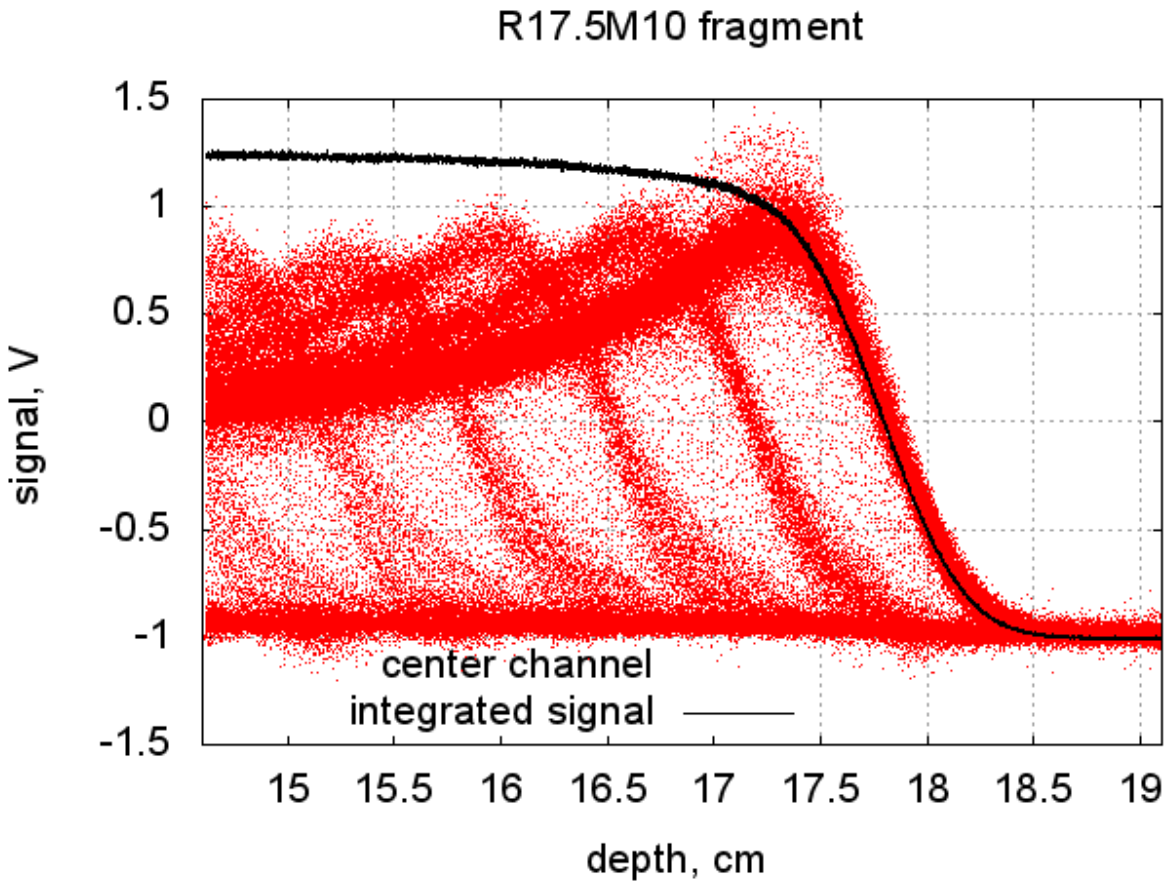

We now compare the SOBP we measured with Geant4 simulation results. That is shown in the next figure. The simulated SOBP was normalized to 1 in mid-SOBP. The measured data was normalized to the simulated data at the shallow end of the measured data (approx 15 cm). We are not yet attempting absolute dosimetry with the chamber. Relatively the agreement is good. We need to collect the rest of the SOBP and will do that soon.

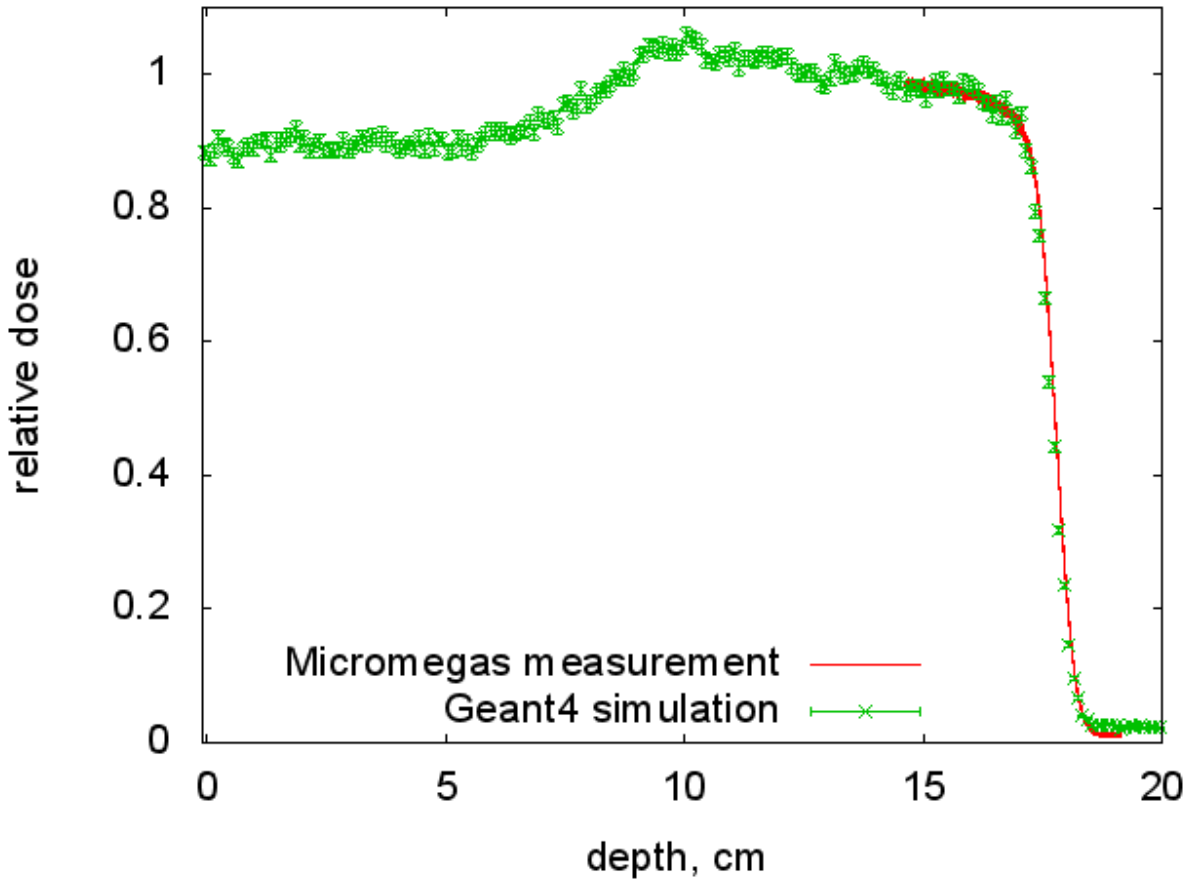

Our measured data is sampled at 1 ms rate. The modulator wheel rotates at 10 Hz, and so you can zoom in on the collected SOBP data and resolve the dose rate variation at any depth produced by the modulator wheel. The next figure is a closeup of the data at about the 600 s point. The first segment of the wheel takes about 29 ms to pass. You are seeing mid-level entrance dose at this depth for that segment. The 5 segment is producing a Bragg peak at this depth, so it the dose rate peaked there. Then the dose rate falls because you are seeing exit dose from the more proximal Bragg peaks. The cycle repeats at 10 Hz.

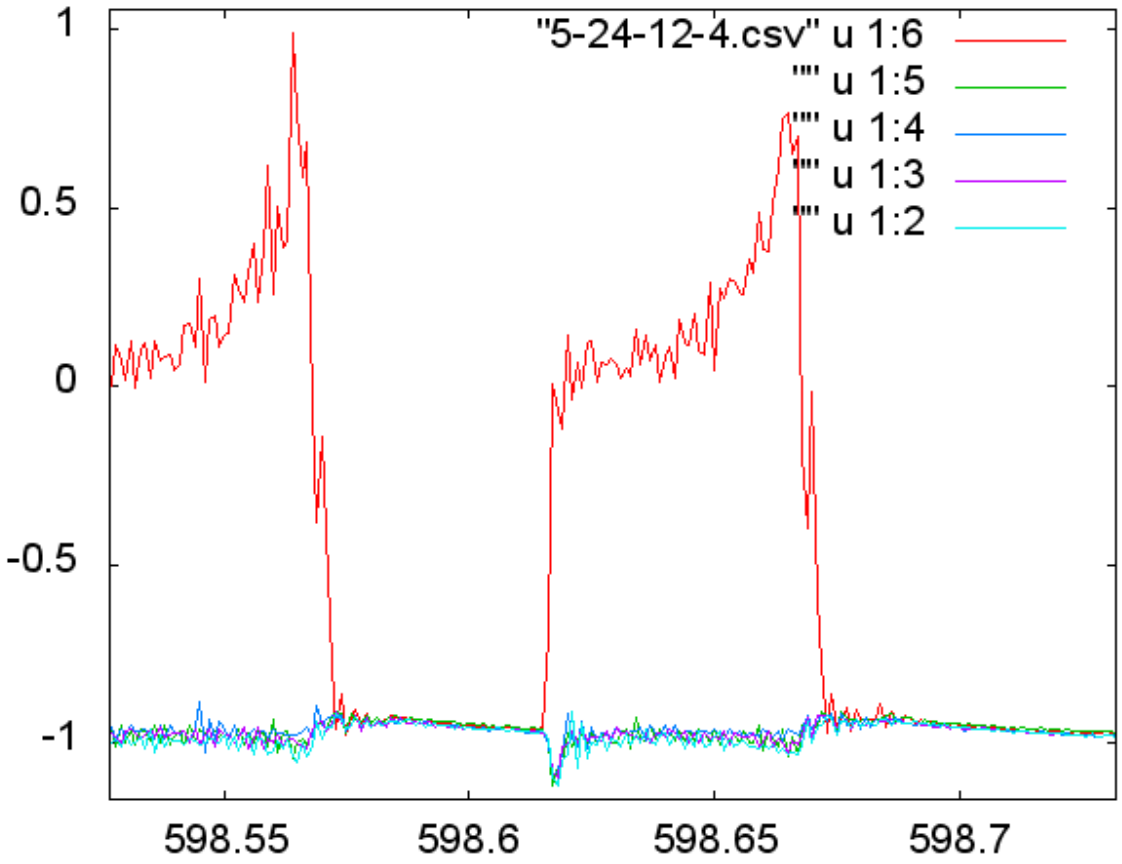

The next figure is a Fourier transform of the SOBP data. The modulator wheel rotation is evident at 10 Hz and harmonics. We use this as a measurement of the modulator wheel rotational frequency. Our measurement is 10.007 +/- 0.002 Hz.

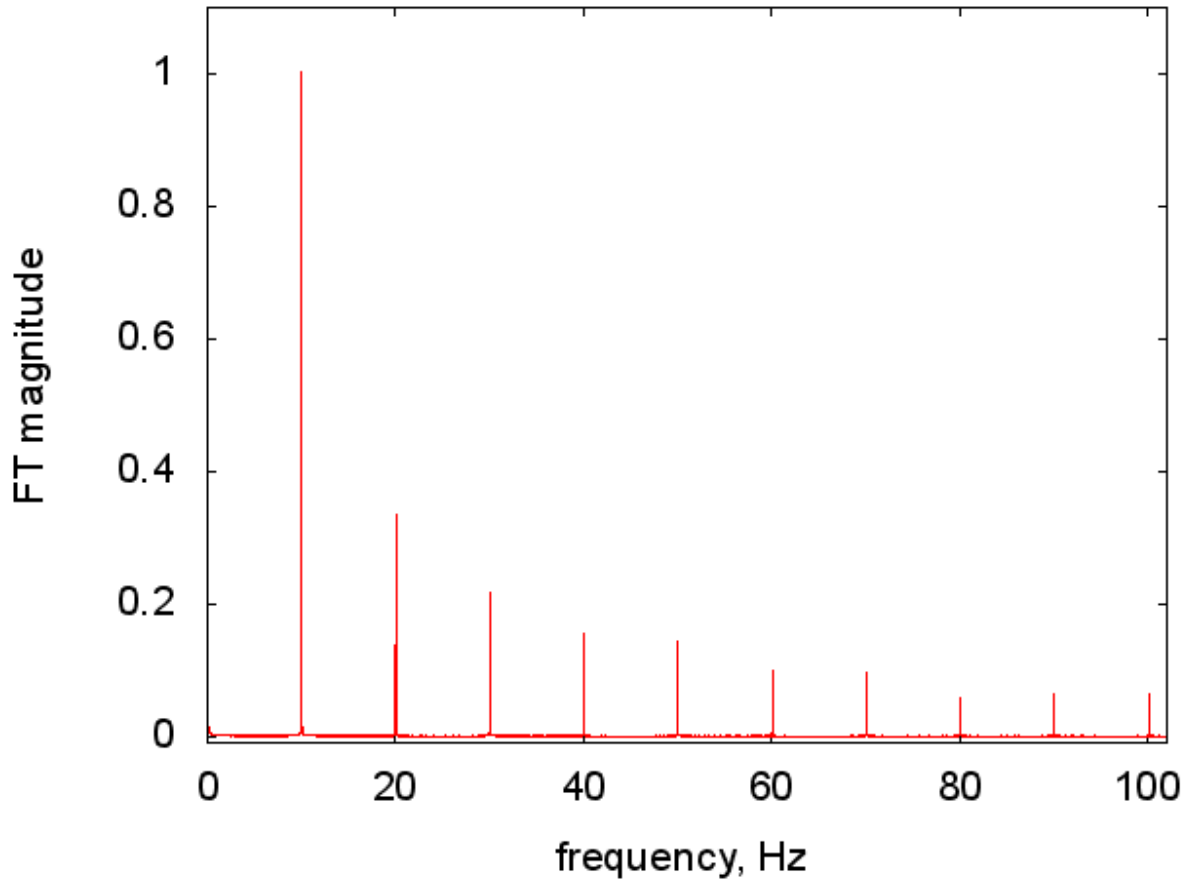

Using that frequency, we have extracted the first Bragg peak from the SOBP data by averaging the signal over the first 20 seconds of the dose pulse. That extracted signal is compared with a Geant4 simulation of a pristine peak delivery (just simulating the first segment of the R17.5 M10 delivery). The results are close. We are getting the entrance dose wrong and we suspect that it is due to the lower energy protons in the nozzle that Maura incorporated into simulation last year in order to fit the commissioning data. The low energy protons were not included in these simulations. We will run simulations with the low energy fit that Maura found to give good agreement with open field data, but we will also obtain an independent measurement of the Bragg peak for this small field using another calibrated chamber scanned in a water tank. Alternatively, the Micromegas chamber may be quenching in the high dose rate in the Bragg peak (the curves are normalized to the peak), and so our measurements and simulations next quarter will be designed to decide test which is the correct explanation.

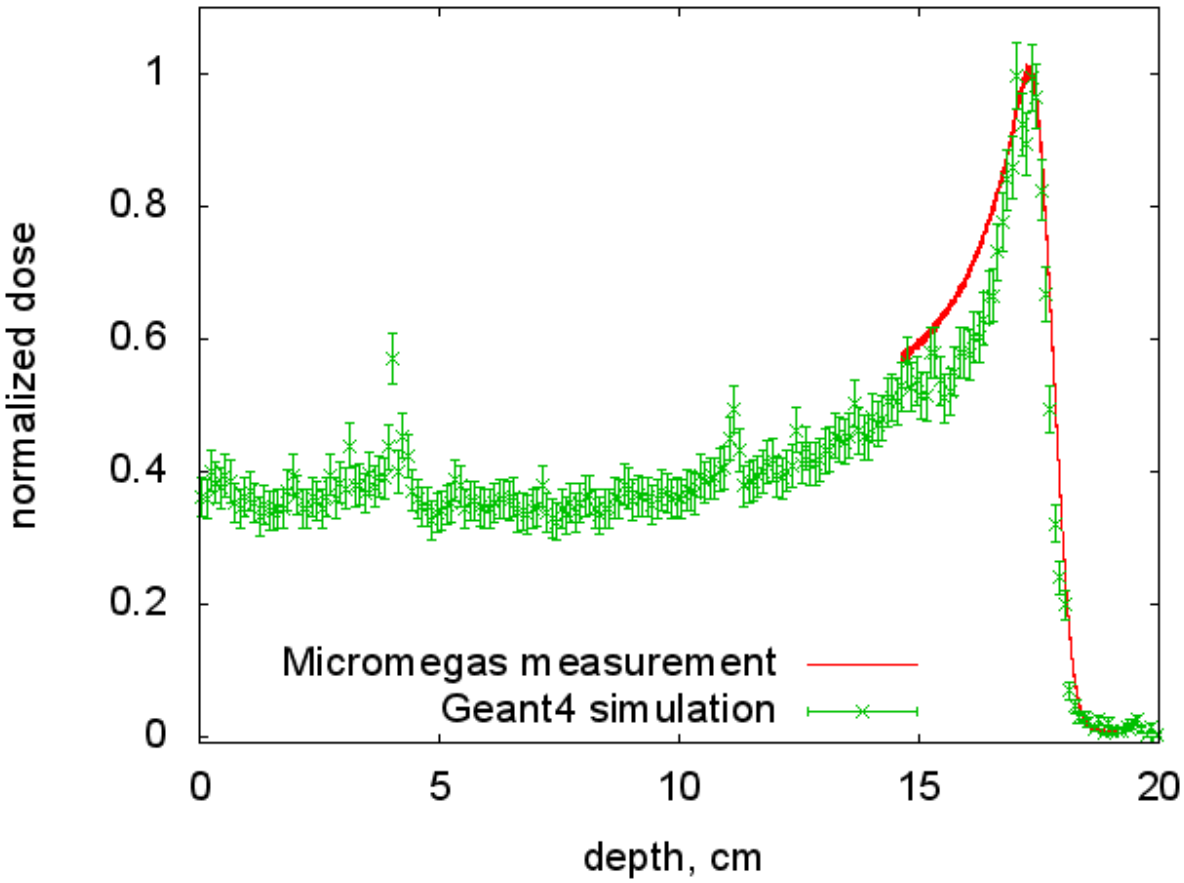

We also collected data of a small spot, 5 mm x 5mm, where the couch was moved between proton deliveries. We slowly moved the small spot across the boundary between the center channel and one of the outer quadrant channels. This data will be used to measure the spatial resolution of the Micromegas chamber.

CERN Micromegas Board

In Q1, we completed the first design of a pad detector which will be mated to a drift region and a MicroMegas amplification plane. The pads are 5x5 mm. The eventual design will have a pad size between 5x5 and 3x3 mm. Position resolution for the 5x5 design will be approximately 1.4 mm or 0.86 for the 3x3 configuration.

The board layout consists of a 10cm array of pads and a four layer board to bring the pad signals out to the connectors. The figure below is a rendering of the PCB with each layer drawn in a different color. The Micromegas and drift planes sit on top of this PCB board.

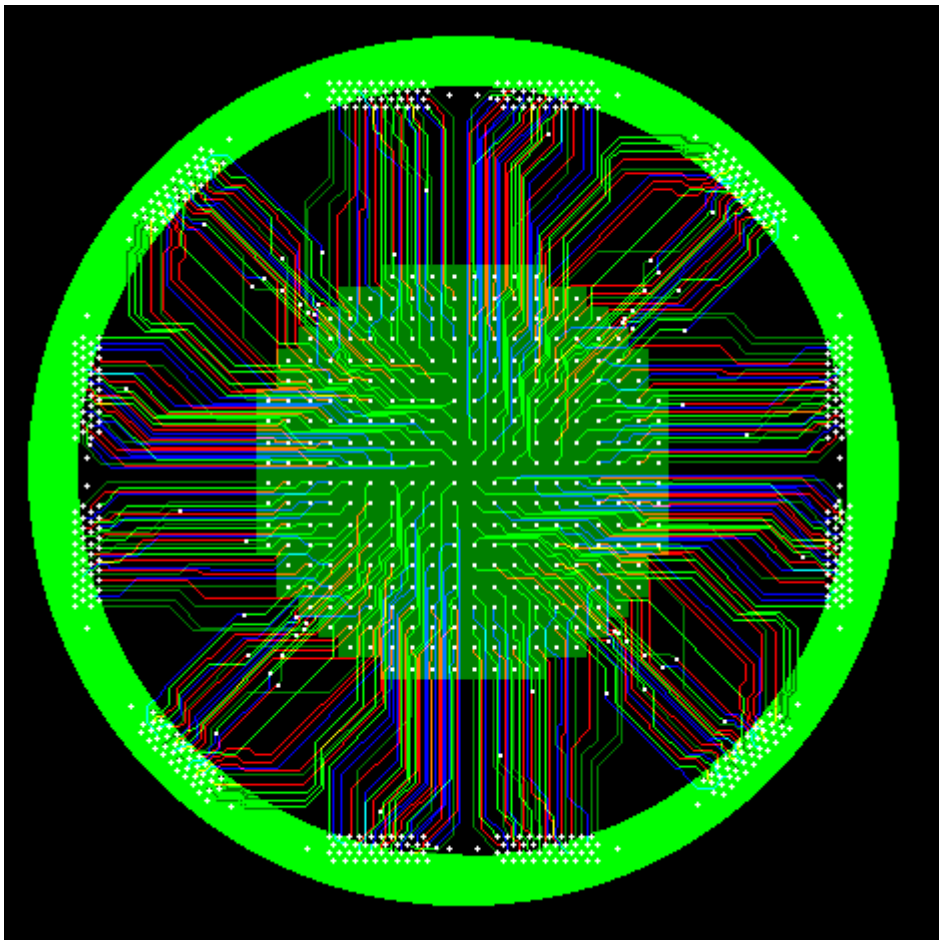

The second figure shows an expanded view of the pad structure on the top layer. The mechanical structure for this is being fabricated and arrangements have been made to send the completed sub-structure to CERN who will manufacture the Micromegas plane in Q2.

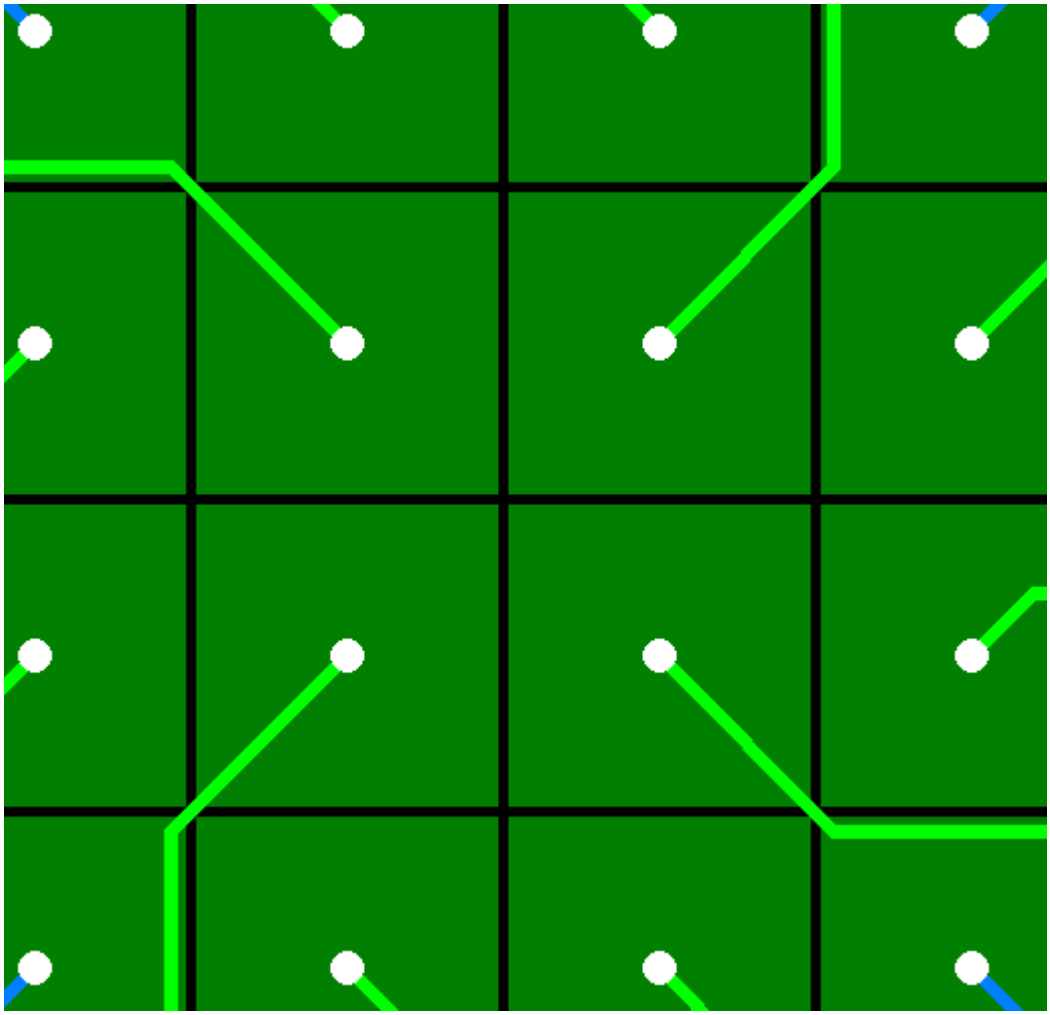

The pixellated Micromegas design has been sent to CERN and was reviewed by the CERN electronics engineer who found some minor problems with the board design. There was a short circuit found and an o-ring was located on top of a high-voltage feed. These issues have been corrected and the prototype is being fabricated. We estimate delivery in 6 weeks.

Milestones Status

This Micromegas proton monitor project began in 10/2011 and so has now completed 3 quarters of research. We believe we are on track with the milestones initially proposed. With respect to the original Q1 milestones, we have measured the gain of the single gap prototype using electrons (reported previously). We measured a pristine Bragg peak using an unscanned beam with the modulator wheel stopped using solid water. We did not measure a double-scattered PDD with the single channel prototype, which was a milestone, because the Micromegas pilot device was available and so we have just finished measuring part of an SOBP with that device. The measurement was successfully and we intend to collect the full SOBP next quarter. We have validated the gain settings for 2D: we can measure Bragg peaks in high-gain mode. We have agreement between the gain we measured in the proton beam and the gain we measure using the test iron-55 source. We have not measured a 2D beam profile yet because we do not have the pixellated CERN prototype yet (coming next quarter), but we have data where the beam is slowly stepped between channels (for a spatial resolution determination),

and we have data of a uniform-scanned beam that shows the beam sweeping from one channel to another and we have measured the beam scanning rates to agree with what IBA says are the rates. We will measure a 2D profile when the pixilated chamber arrives. For the 3D device, we have design the readout electronics, the PC interface, and the frontend PC software. We have validated this data readout chain with the 5-channel CERN pilot device. The detector has been implemented in simulation, both Geant4 Monte Carlo simulations for proton beam simulations, and Garfield for simulations to determine the electromagnetic field within the chamber under different geometries, voltages, and gas compositions.
We have still to make choices about the buildup material that will provide overall tissue equivalence. This will rely on Geant4 simulations and we expect to complete that study next quarter. We have measurements of the single-layer gain from the CERN pilot device. The layer spacing in this device is the same as the final pixilated chamber, and so we do not expect the gain to be any different. We have not measured a PDD with the final pixilated chamber, but we have a measurement using the pilot device with a narrowly-collimated beam that provides the same proton flux per channel, and so we believe our SOBP measurement with the pilot device is relevant, and we will finish the comparison of that measured data with simulation and a calibrated ion chamber measurement next quarter.
Due to time constraints we decided to make the first pixilated prototype design smaller than we had hoped. CERN will manufacture a 10x10 cm2 prototype rather than the 20x20 cm2. This reduces the number of pads to readout, so that we do not need to assemble so many readout boards, but also so many pads would be 7 or 8 PCB layers to bring all the signals out from the active area, and would take longer to design. The smaller prototype will nevertheless prove the feasibility of this technology, and would be still be somewhat useful even if it could not be used to verify the largest treatment fields in one acquisition. After having validated the PCB circuit design with Spice simulations, we have finalized the design for the pixilated CERN fabrication and it has been sent to CERN and we should have the first production prototype next quarter.

II. Development of a Scanned Proton Beam System for Proton Radiotherapy

Proton room 2 commissioning and validation was completed last year and we were now treating about 10 patients per day in the room with PBS. But the scanning magnet power supply system (SMPS) failed and we lost room 2 for two months. The SMPS has been repaired by IBA and the room is running again. In addition the scanning magnets were upgraded to a newer (quieter) design. We now have to re-collect a subset of the commissioning data to validate that the system has not changed with respect to the beam dosimetery. That re-validation is underway.
We had started PBS commissioning in room 3. We had collected all Bragg peaks and beam profiles in air. Validation was not complete at the time that the SMPS went down. The room 3 commissioning is on hold until room 2 is re-validated, and will restart after that time.
Derek has used the collected phase space data to generate an initial phase space for simulations with starting point upstream in the treatment nozzle. That procedure has been mostly described in previous reports: the beam spot profiles are corrected for multiple scattering in air by computing the scattering contribution to the spot size as calculated with Geant4, and a quadratic as a function of depth in air is fit to the resulting spot sigmas. This quadratic function thus represents the simple geometric beam optics that would determine the spot size were it to propagate in vacuum. The initial spot size and beam divergence are determined from the polynomial coefficients. The difference in the case of fitting the commissioning data is that we have the spot size at 7 or 8 air depths to use to fit the quadratic. Previously we relied on IBA spec for spot size at isocenter, measurements of the beam emittance at another facility, and the idea that the beam would be focused at isocenter to determine the 3 parameters of the quadratic. It turns out that the beam is not focused exactly at isocenter, but it does not matter.

The data is fit well by a quadratic function, which indicates that Geant4 is calculating the multiple scattering well enough in air, at least. The measured spot size in air is compared with Monte Carlo simulations in Figure II-1.

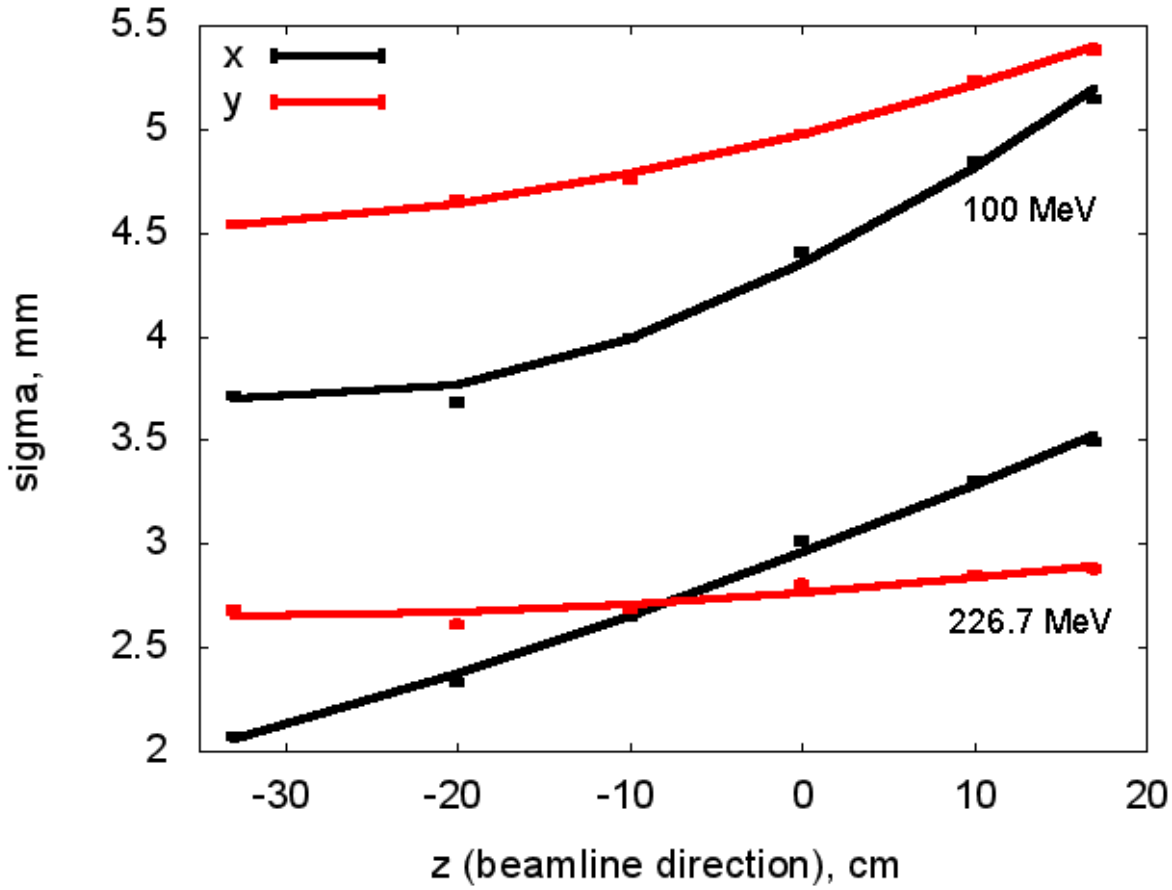

Figure II-1. Comparison of Monte Carlo (lines) beam profile in air with data (points) measured during commissioning. Shown here are the maximum and minimum beam energies. The range shifter is not in the beam line.

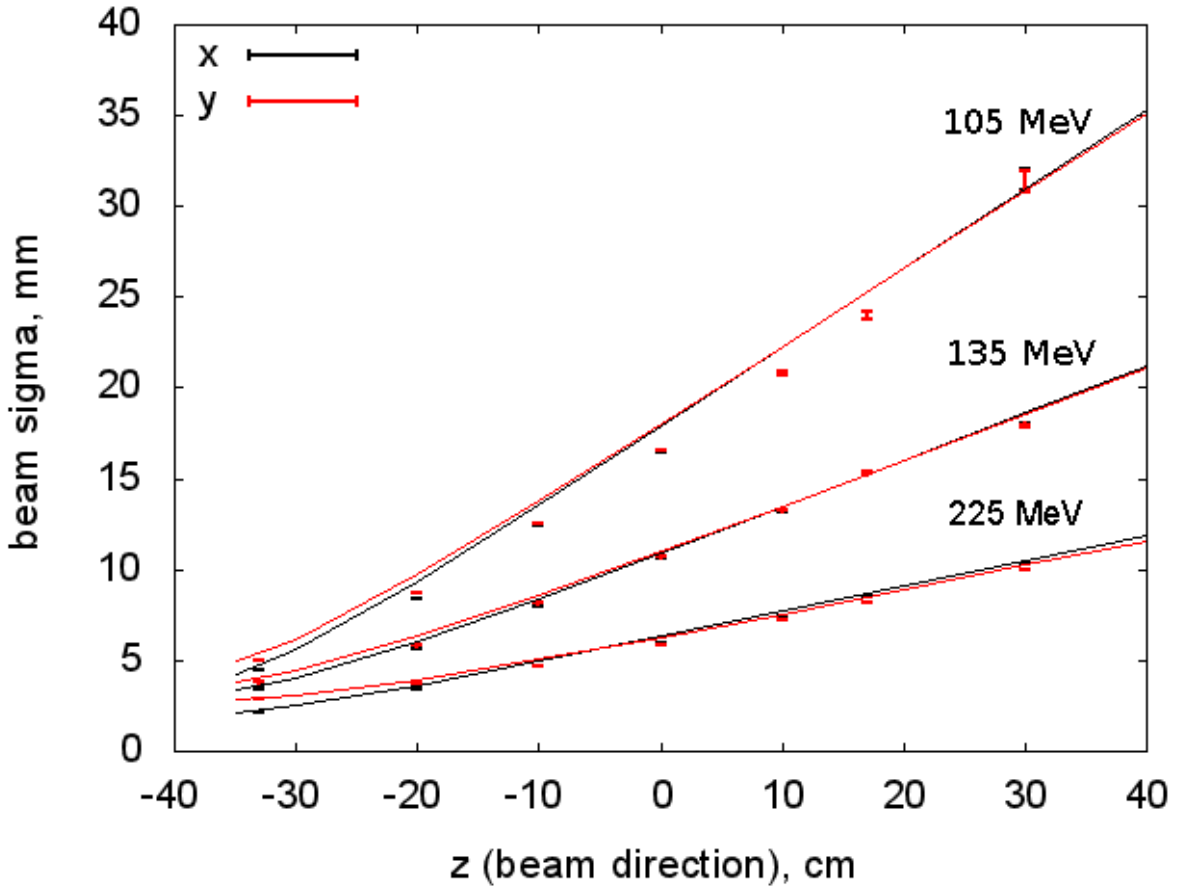

Figure II-2. Comparison of Monte Carlo (lines) calculated beam profile with measured (points with error bars) data using the range shifter collected during Room 2 commissioning. The initial phase space for Monte Carlo was obtained from fit to the open beam commissioning data.

We have also verified that Geant simulations reproduce the spot size when the range shifter is used. The beam profiles measured with the range shifter were not used to produce new fitting functions. The same initial phase space that fits the open beam case also reproduces the spot size for the case of the range shifter, indicating that Geant is modeling the scatter in the range shifter well enough. The comparison of spot size measured and simulated for the range shifter case is shown in Figure II-2.

We have now begun to compare measured depth-dose curves with simulation. A comparison of the lowest and highest energy beam are given in Figure II-3. There is some difference in the shape of the Bragg curve particularly the slope in the entrance region. We are investigating the origin of this difference at present. One possible effect contributing to the difference is that we are not collecting all of the charge deposited in the water phantom due to the finite size of the Bragg Peak chamber. A long dose tail is produced by multiple Coulomb scattering and nuclear interactions, and when many spots are summed to produce a uniform dose to s target, the tail accumulates to produce a so-called dose halo around the target. The dose tail can grow larger than the diameter of the chamber (8 cm). Some evidence for this can be seen in the commissioning measurements: the dose collected with a the beam scanning a large uniform

field appears to be about 10% larger than that measured with a chamber attempting to integrate the full dose profile of an unscanned beam. Unless the treatment planning system can be made to model the dose halo accurately, it may be necessary to implement field-size dependent corrections to the dose per MU. It is our intention to further investigate the difference between the Monte Carlo-simulated Bragg peaks and the measured data next quarter.

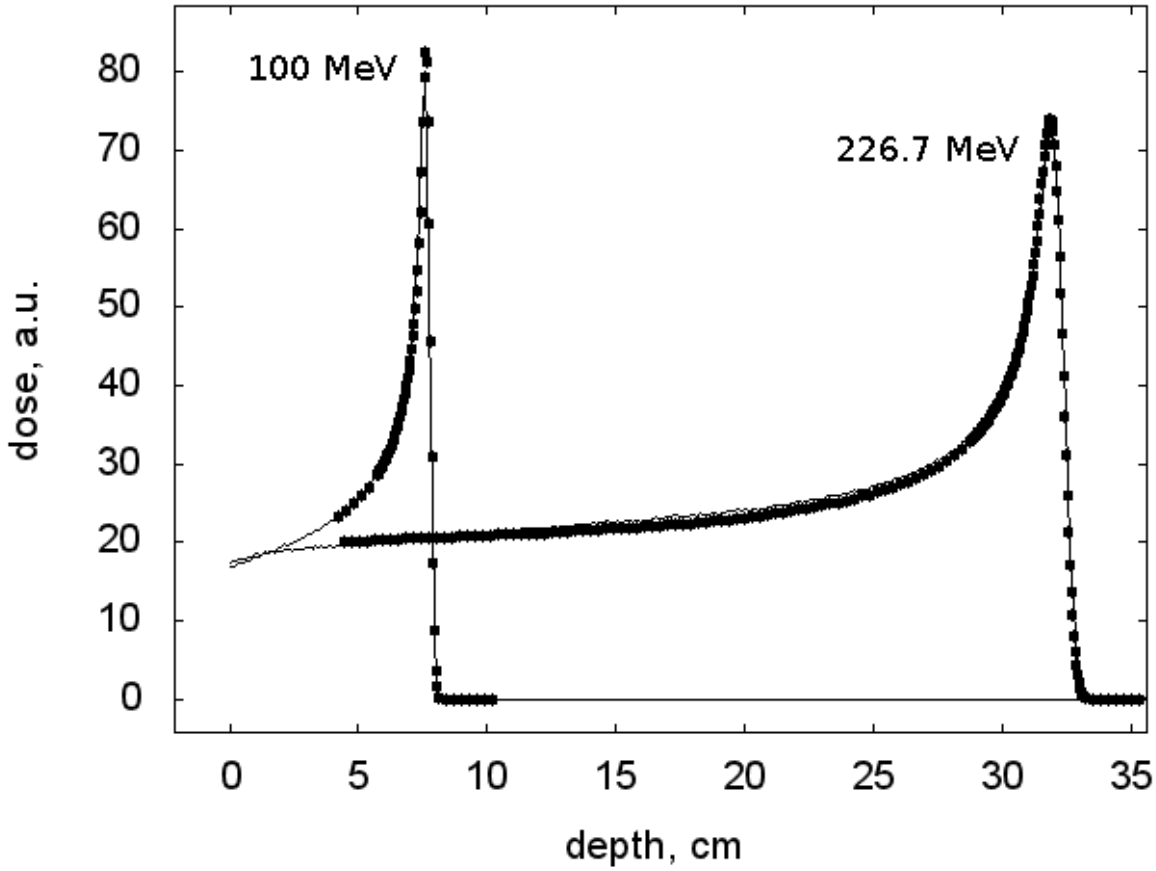

Figure II-3. Comparison. of Monte Carlo (lines) generated depth dose curves with measured (points) data collected during Room 2 commissioning.

Derek has migrated the DICOM dose output code from Imebra to GDCM. Imebra is very slow to write multi-frame image files, of which RT Dose files are one kind, because when it inserts each new frame into the file, it performs a memory copy of all of the old ones. The Imebra developer was contacted. He acknowledged the issue but said that he did not have time to completely fix the issue in the near future. He did suggest a possible workaround. Instead, Derek tried a different open-source DICOM toolkit called GDCM. This is a mature project with good documentation and is distributed with many good examples. Derek re-implemented the DICOM dose output using GDCM instead of Imebra. Whereas the old code using Imebra took > 4 hrs to write a DICOM dose file with 200 slices, the new implementation using GDCM takes about 30 seconds. The old implementation was an annoying bottle-neck in the simulation workflow for several projects at Penn. The new implementation is now being used by Eric Diffenderfer and Maura Kirk as one of the steps in the simulations they are running for other projects.

Derek is using the original room 2 validation data to validate the Geant4 Monte Carlo PBS code. That is a prostate field. In addition, ring patterns were constructed and delivered to film. These patterns amplify the small dose in the tails of the beam profile where some non-Gaussianity from large-angle MCS and nuclear interactions is observed at other centers. Derek is comparing the Monte Carlo dose calculation with the Eclipse calculated dose and the dose measured with film and the Matrixx device for the “johndoe” validation plan. The Monte Carlo vs. Eclipse comparison is shown in the following figure. The Monte Carlo simulation was run using the Eclipse plan file, simulating only 300,000 protons per target in the plan. There were a total of 2843 targets for this field. The phantom material was water in the simulation, and in Eclipse the material in the body contour was set to water. A dose profile was extracted from the Monte Carlo dose cube at a depth 24.2 cm, and a dose plane of the same depth was exported from Eclipse. The dose Monte Carlo dose was not normalized to the level of the Eclipse dose: the absolute dose is fixed by simulation of the same 10 cm x 10 cm x 10 cm (R18M10) plan that was used for the absolute output measurement in following the TRS-398 protocol. The number of protons per MU for simulation was fixed so that the dose at the center of the cube agrees with the dose measured with an FC65 farmer-type chamber. Also shown in Figure II-1 is a gamma comparison using 3% and 3 mm thresholds. The number of pixels failing the gamma test is 14%. As reported previously, we initially thought the problem was due to large statistical noise, but this is a run with a very large number of events (300k events/kernel). As can be seen in the lower right plot in the next figure, the gamma analysis is failing in the beam penumbra, but primarily failing along the Y direction and not so much in the Z direction. Our latest hypothesis is that this is due to the large voxel dimension in the Y direction. The Y direction corresponds to the slice direction of the CT data. The slices are 2.5 mm thick. The same voxel dimensions are used to score the dose so in fact the dose grid is rather large in the Y direction. You can see that part of the voxel passes gamma comparison with the film, but the falloff gradient is steep enough that a significant fraction of the voxel fails the 3%/3mm comparion criteria. Derek wrote some code to generate a dose grid with finer resolution than the CT dataset, and is now running the johndoe plan with uniform 1 mm x 1 mm x 1mm voxels to test this hypothesis.

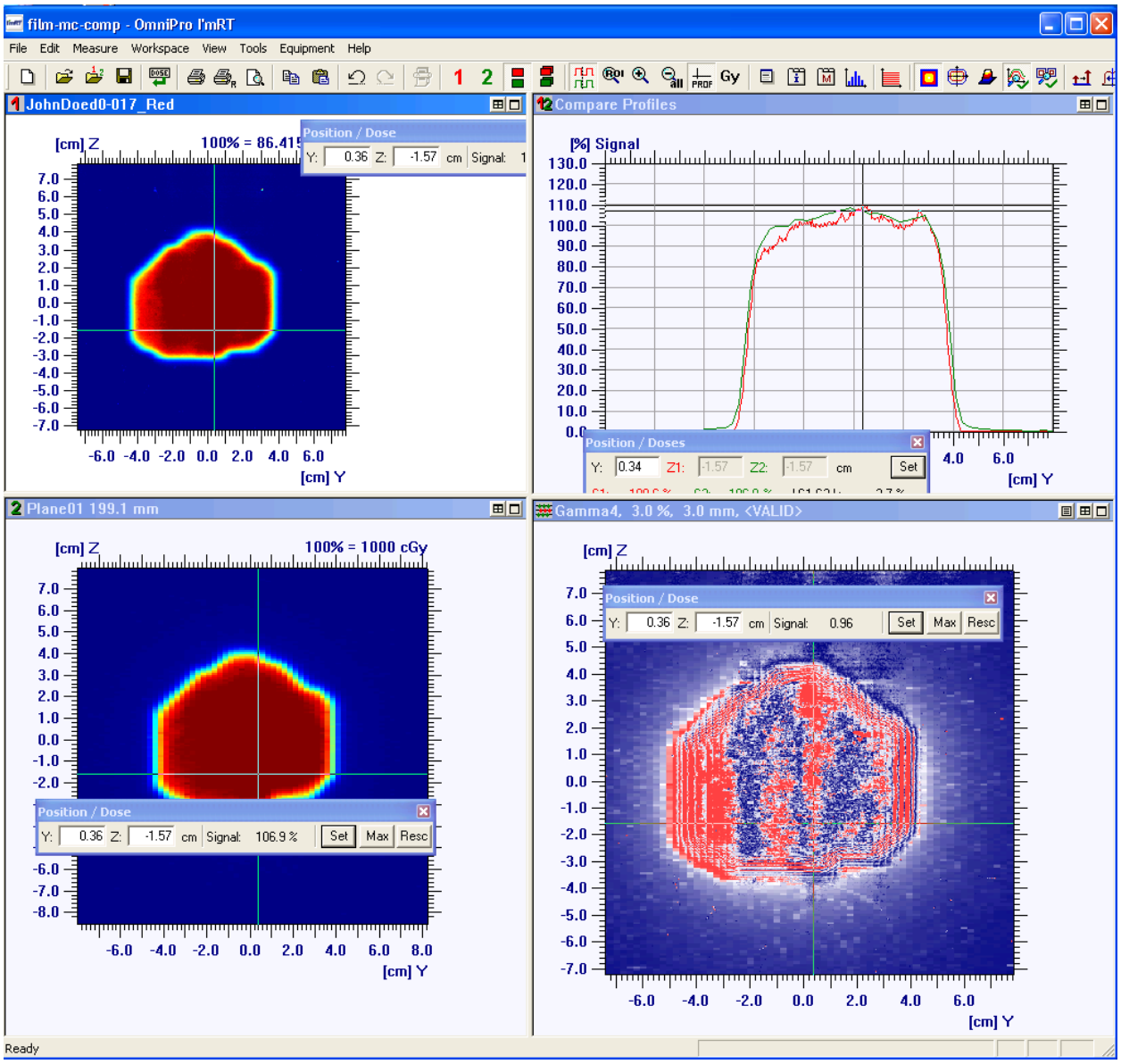

Figure II-4. Comparison of Eclipse-calculated and Monte Carlo-calculated "johndoe" prostate field used for Treatment Room 2 validation. Upper left is the Eclipse-calculated dose, lower left is the Monte Carlo-calculated dose. Lower right is a gamma comparison between the two plans: 14% of points in the region shown fail 3% by 3mm gamma (there is no low dose threshold).

Besides the johndoe plan, some plans were created with Eclipse to deliver dose rings. The point of the ring is to amplify the low-dose halo that is expected to be present around the primary Gaussian spot profile. The dose halo should be understood because it can make the dose per MU field-size dependent, and can complicate the measurement of Bragg peaks since the full dose profile is not collected even by the relatively large Bragg peak chamber. In Figure II-2, Derek compares a dose ring film measurement with Monte Carlo calculation. For this plan, the Monte Carlo dose was normalized to agree with the film measurement in the peak. This was done because the absolute dose delivered to film is not known: the MUs were adjusted at

delivery time by modifying a PLD file to maximize dose resolution of the peak and the center (halo) region. The number of MUs was chosen be high enough so that the low dose halo could be measured in the center of the ring, but not so high that the film saturated in the relatively high dose region of the ring itself. This plan was delivered and simulation through the range shifter, which was expected and observed to produce the largest magnitude halo. The Monte Carlo does not quite have enough dose in the halo: it is only 3% relative to the ring dose, as opposed to the 5% that you see in the measured data. It is believed that this is due to the fact that the beam monitor chambers are not included in the simulation. These are multi-layer transmission ionization chambers with very thin layers but that are nevertheless high Z materials that will scatter some protons at large angles. Because they are upstream, the scattering angle need not even be very large to deliver dose far off axis. Derek will implement the monitor chambers in the Monte Carlo nozzle code and check for better agreement with the dose ring measurements.

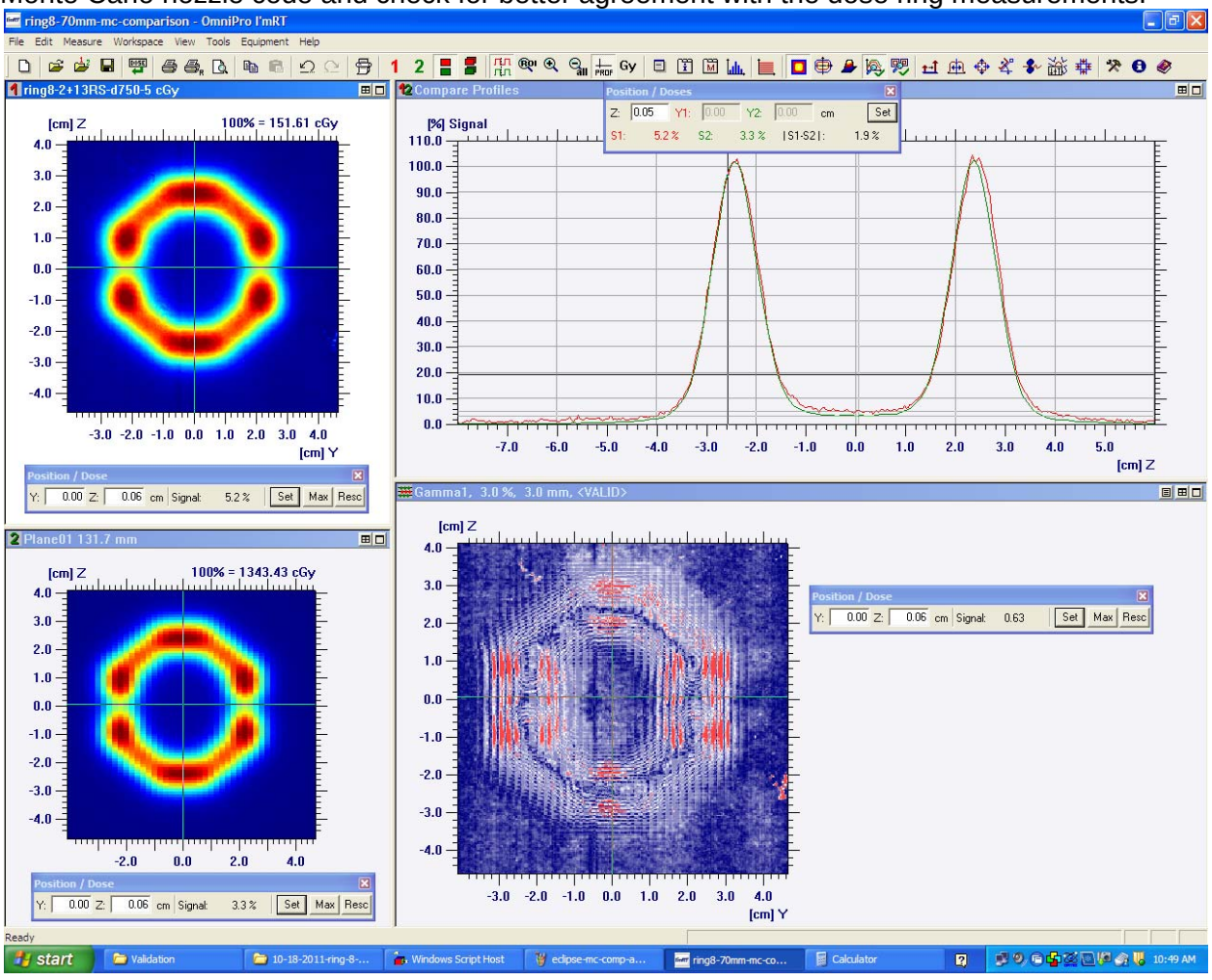

Figure II-5. Comparison of film measurement (top left) with Monte Carlo simulation (lower left) for a dose ring. The point in the center of the ring receives a low dose contribution from the halo around all the spots delivered around the ring. The Monte Carlo halo dose is a few percent lower than the measurement.

III Adaptive Radiation Treatment for Changes in Tumor Motion and Volume

OVERVIEW

In recent years, conformal techniques have been developed that allow for precise delivery of radiotherapy to the primary tumor and regional lymphatics while minimizing the dose to normal tissues. These approaches are predicated upon precise anatomic localization of the regions to be irradiated. Unfortunately, at present, most conformal treatment delivery approaches do not account for changes in tumor volume, tumor motion or changes in patient anatomy during the time course of definitive radiotherapy. Proton beam radiotherapy can potentially allow for ultra-precise delivery of treatment due to the physical characteristics of the proton beam. Therapeutic proton beam radiotherapy allows for the elimination of exit dose and a significant reduction in the entrance dose to the patient while maximizing dose delivered to the tumor (Figure 1). However, accurate treatment delivery with proton beam radiation is predicated upon precise definition of tumor volume and location. Tumor volume reduction during definitive proton beam radiotherapy has resulted in significant dosing errors, with dose deposition in unintended regions (MDACC PTCOG 47). The purpose of this protocol is to quantify the extent of tumor volume, motion, and anatomic changes that occur during the tumor course of definitive photon beam radiotherapy. As both proton beam and photon beam radiotherapy have nearly identical biological efficacy, the changes observed during photon beam radiotherapy should closely approximate that which would likely be observed during proton beam irradiation. The long-term goal is to use this data to develop an adaptive treatment approach for proton and photon beam radiation.

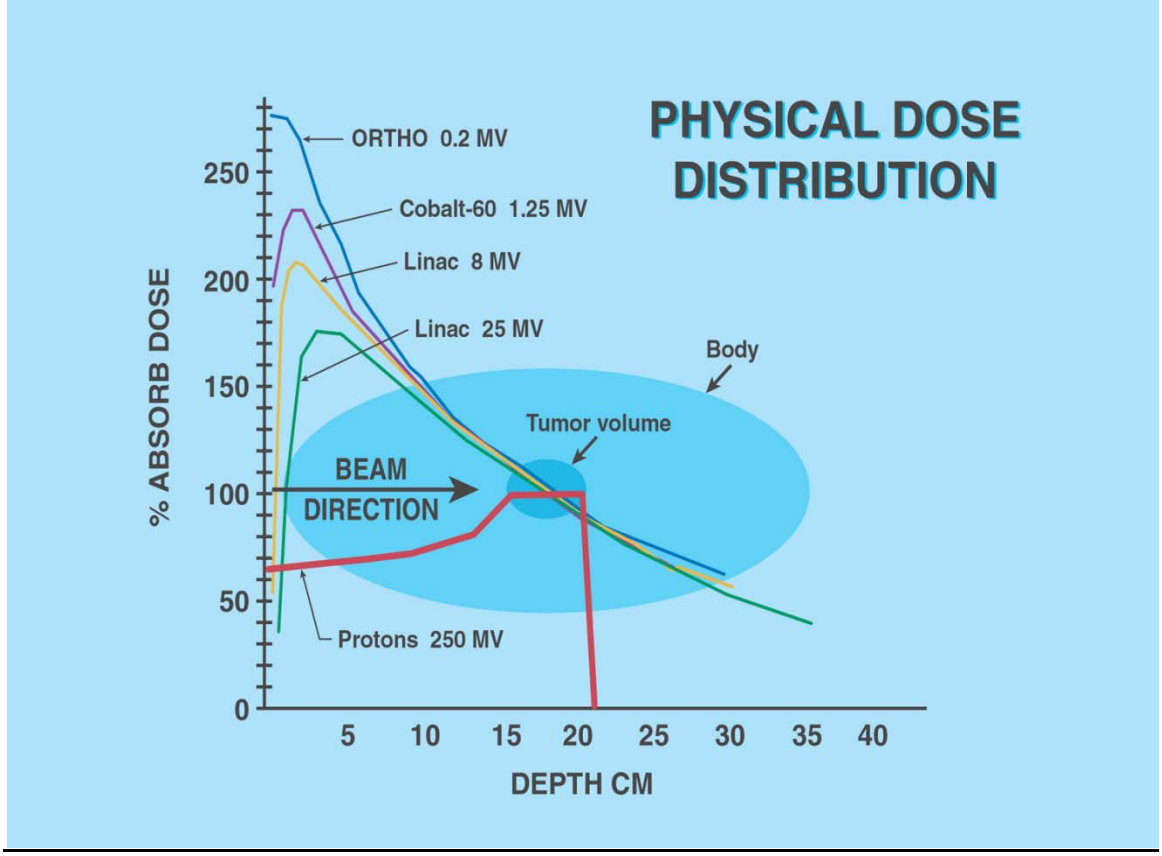

Figure 1: Comparison of Dose Deposition between Photon and Proton Beam Radiotherapy

SPECIFIC AIMS/OBJECTIVES

Overall Aim
To estimate the degree of tumor volume, tumor motion, and patient anatomy changes that occur during the time course of definitive photon and proton beam radiotherapy. To use the data obtained in this study to ultimately develop an adaptive radiotherapeutic approach that accounts in fast dose calculation engine to allow for adaptation to account for these changes

Primary Aim
To estimate the degree of tumor volume, tumor motion and patient anatomy change during treatment with photon beam radiotherapy using weekly 4D or 3D CT Scans and use this data to develop a fast dose calculation engine to allow for treatment adaptation.

Secondary Aims
To estimate the degree of tumor volume, tumor motion and patient anatomy change during treatment with proton beam radiotherapy using weekly 4D or 3D CT Scans

Progress this quarter:
The protocol received Penn IRB approval to open for recruitment in November 2009 and is expected to complete accrual in November 2014. The protocol enrollment goal is 120 subjects with 30 patients per stratum (e.g. gynecologic cancers). As of June 2012, enrollment is at 60 subjects (50% complete): 9 GI, 22 gynecologic, 3 head and neck, and 26 lung patients. There have been no protocol deviations or serious adverse events to date.

Image quantification on the accrued data sets has begun. Data analysis will strive to analyze the effect of tumor changes and patient anatomy changes on radiation treatment efficacy and will be initiated once contours are complete on current patients. To date, contouring has been completed for 42 of 60 patients. Contouring for the remaining patients will be completed by the end of October 2012. Once contouring is complete tumor volume and motion data will be tabulated and analyzed by Dr. Kevin Teo.

Preliminary data analysis may be completed in time for abstract submission to the American Society of Clinical Oncology in early 2013.

Key Research Accomplishments

The major accomplishment of the past year has been the successful introduction of Pencil-Beam-Scanning in the fixed beam room and the related commissioning of the Eclipse planning system. The prototype detector development and the use of PBS in the gantries are on-going.

A second accomplishment has been the robust growth in clinical treatment protocols for our patients. There are currently 15 IRB-approved proton therapy protocols accruing patients at our center. A total of 812 patients, 642 adults and 170 pediatric patients have completed proton treatment as planned. At present, on treatment there are 60 adults and 13 pediatric patients for a total of 73 patients.

Reportable Outcomes

The following papers based on work performed on this project have been accepted during the past year:

- Belard A, Dolney D, Tochner Z, McDonough J, O'Connell J: Improving Proton Therapy Accessibility Through Seamless Electronic Integration of Remote Treatment Planning Sites. Telemedicine and e-Health 17: 370, 2011.
- Eric S. Diffenderfer, Christopher G. Ainsley, Maura L. Kirk, James E. McDonough, and Richard L. Maughan: Comparison of secondary neutron dose in proton therapy resulting from the use of a tungsten alloy MLC or a brass collimator system. Med. Phys. 38: 6248-6256, 2011.
- Rulon R. Mayer, Fuhwa Ma, Yu Chen, Rachel I. Miller, Arnaud Belard, James McDonough, and John J. O'Connell: Enhanced dosimetry procedures and assessment for EBT2 radiochromic film. Med. Phys. 39: 2147, 2012.
- Simone CB 2nd. Kramer K. O'Meara WP. Bekelman JE. Belard A. McDonough J. O'Connell J.: Predicted rates of secondary malignancies from proton versus photon radiation therapy for stage I seminoma. International Journal of Radiation Oncology, Biology, Physics. 82(1): 242-249, 2012.
- Yu Chen, John J O'Connell, Christine J Ko, Rulon R Mayer,Arnaud Belard1, and James E McDonough: Fiducial markers in prostate for kV imaging: quantification of visibility and optimization of imaging conditions. Phys. Med. Biol 57: 155-172, 2012.

Conclusions

This report documents the work that has been accomplished during the seventh year of the project to design an MLC for proton radiotherapy, the sixth year of work on the scanned beam project, and the fifth year of work on the image-guided proton therapy project. It concentrates on the past quarter since reports on the other quarters already have detailed those efforts. Together with our colleagues at WRNMMC we continue to develop the telemedicine component including remotely operating the treatment planning system. In addition the WRNMMC group extended their studies of the effect of inhomogeneity and organ motion.